Advanced processing methods to introduce and preserve dipole orientation in organic electro-optic materials for next generation photonic devices

Su Huang

A dissertation submitted in partial fulfillment

of the requirements for the degree of

Doctor of Philosophy

University of Washington

2012

Reading Committee:

Professor Alex K.-Y. Jen, Chair

Professor Fumio Ohuchi

Professor Peter Pauzauskie

Program Authorized to Offer Degree:

Materials Science and Engineering

DEDICATION

To my dear wife, daughter, and parents.

ACKNOWLEDGEMENTS

First of all, I would like to thank my advisor, Professor Alex Jen, for giving me the opportunity to join his group and work in the exciting field of organic nonlinear optical materials. His encouragement, support, and guidance have accompanied me throughout my Ph.D. study. I also want to thank my committee members, Dr. Fumio Ohuchi, Dr. Rene Overney and Dr. Peter J. Pauzauskie for their time, effort and advices.

My group leader, Jingdong Luo, together with Dr. Zhengwei Shi, Dr. Xinghua Zhou and every current and former NLO group member has also given me tremendous help in the past 6 years. I do feel very grateful and will not forget about that. I want to express the same gratitude to many current and former Jen group members, especially Dr. Steven Hau, Dr. Orb Acton, and Dr. Angus Yip, for their very helpful suggestions and advices.

I would also like to thank the groups of Dr. Antao Chen, Dr. Michael Hochberg and many other collaborators for the help and support provided in numerous collaborations. Together we accomplished a lot of exciting achievements.

My deepest appreciation belongs to my family. Without their unconditional love and unending support through the years, I would not have been able to go this far.

ABSTRACT

Title: Advanced processing methods to introduce and preserve dipole orientation in organic electro-optic materials for next generation photonic devices

Author: Su Huang

Advised by: Professor Alex K.-Y. Jen

Organic electro-optic (E-O) materials have attracted considerable research attention in the past 20 years due to their rising potentials in a lot of novel photonic applications, such as high-speed telecommunication, terahertz generation and ultra-fast optical interconnections. In order to gain the Pockels effect based E-O activity, the centro-symmetry of amorphous organic E-O materials needs to be removed by a poling process, which introduces orientation to the polar chromophores by applying high electric field. After poling, this collective orientation is subject to a slow decay over time, which can eventually dissipate the E-O activity of the poled material. Thus the study of how to effectively introduce and preserve chromophore orientation forms an important part of the research of organic E-O materials.

This dissertation starts with a general introduction to the field in Chapter 1, which includes the basic nonlinear optics, the design rules for material development, and the potential applications as well as the motivation and scope of this dissertation.

Chapter 2 of this dissertation focuses on a barrier layer approach to improve the poling efficiency of E-O polymers. First of all, high conduction current from excessive charge injection is identified as a fundamental challenge of effective poling. After analyzing the conduction

mechanism, we introduce a sol-gel derived thin titanium dioxide (TiO_2) layer that can significantly block excessive charge injection and reduce the leakage current during high field poling. Ultralarge E-O coefficients, up to 160–350 pm/V at 1310 nm have been achieved by poling with such a barrier, which are 26%–40% higher than the results poled without such a TiO_2 layer. This enhancement is explained by the suppressed charge injection and space charge accumulation by the insertion of the high injection barrier from the TiO_2 barrier layer.

In Chapter 3, the impact of the inserted barrier layer on the temporal alignment stability of E-O polymers is discussed. Considerable stability enhancement is confirmed using both standard 500-hour temporal alignment stability test at 85 ^{o}C and thermally stimulated discharge method. We suggest that the enhancement comes from improved stability of the screening charge. During poling the additional barrier layer helps to lower the injection and thus the space charge accumulation. And this reduced space charge accumulation further helps to replace the space charge part in the total formulation of screening charge with more stable interface trapped charge. We thus expand this knowledge to a group of other materials that can also block excessive charge injection and suppressed space charge accumulation, including dielectric polymers polyvinyl alcohol (PVA), poly(4-vinylphenol) (PVP) and TOPAS as well as ferroelectric polymer poly(vinylidene fluoride-*co*-trifluoroethylene) (P(VDF-TrFE), 65/35 copolymer), which differ largely from the others in dielectric constant, conductivity and surface properties. The only common feature of them is that they all lowered the charge injection and leakage current for 1-2 orders during poling. On every buffer layer we tried, similar trend of stability enhancement is found. These results suggest that the observed temporal stability enhancement is indeed an effect from the abovementioned mechanism.

Chapter 4 focuses on the development of an innovative new poling method, which utilizes pyroelectric effect instead of external power sources to overcome the limitations of conventional contact poling and corona poling. With careful theory assisted design, we developed a reliable protocol to efficiently introduce dipole orientation in organic E-O materials by heating and cooling them with detachable pyroelectric crystals. This new method can potentially improve the process adaptability of organic E-O materials in a variety of photonic devices. Large Pockels coefficients (up to 81 pm/V at 1.3 μm) have been successfully achieved in thin films poled using this method. The effective fields in these experiments are estimated to be around 0.5 to 0.9 MV/cm, which agree well with the electrostatics analysis using an idealized model. The same method is directly applied to surface modified hybrid polymer silicon slot waveguide ring-resonator modulators devices. A 25 pm/V tunability of resonance peak wavelength shift has been realized, which was higher than any reported results in similar devices.

Chapter 5 discusses about the possible application of the pyroelectric poling in a multi-stack waveguide device architecture. A long-existing challenge to pole E-O polymer based photonic devices is how to effectively drop the poling voltage to the core layer, which is usually sandwiched between two dielectric claddings. In the past, this was done by using relatively conductive claddings, which on the other hand can bring larger optical loss and dielectric loss to the waveguide. Thus careful engineering compromise must be made between better poling efficiency and lower loss. Pyroelectric poling as discussed in Chapter 4 opens up new possibilities. In this chapter, it is demonstrated that E-O polymer films can be poled even with 3 orders thicker dielectric layer in circuit using pyroelectric poling. The theoretical analysis matches well with the experimental results. It could provide new insight to the research of poling

E-O polymers in hybrid photonic devices, where the E-O materials form intimate contact with different types of materials in the system.

TABLE OF CONTENTS

LIST OF FIGURES

LIST OF TABLES

Chapter 1. Introduction

In the past twenty years, the world has witnessed a rapid growth in the research of organic electro-optic (E-O) materials and related device systems. Due to their unique properties, organic E-O materials have shown potential advantages in many novel photonic applications, such as high-speed telecommunication, terahertz (THz) generation, ultra-fast optical interconnection and non-invasive electromagnetic wave sensing.[1-5]

The E-O activity of organic material mainly comes from the movement of π-electrons, which can respond in femtosecond scale. Compared to inorganic materials, which utilize either phonon response or carrier density response as the main mechanism, organic E-O materials have an intrinsic speed advantage of at least 3 orders.[5-6] This underlines one of the most fundamental motivations of the research on organic E-O material. On the other hand, after two decades of intensive studies, modern organic E-O materials have demonstrated one order higher E-O coefficient than the benchmark inorganic material $LiNbO_3$ while at the same time showing much less dispersion, easier fabrication, and potentially lower cost.[2] With all these adavantages combined, organic E-O materials have shown great potentials in a broad variety of photonic applications.

1.1 Nonlinear optics for organic materials

The E-O effect, together with all other nonlinear optic effects, originates from the interaction between light and the optical medium. When light pass through a medium, energy from the light may change the optical properties of that material. On the other hand, if the optical

properties of an illuminated material are changed, this will in turn influence the propagation of light in that material. This is the overall philosophy of all nonlinear optical effects.

If we consider the response of a material to an applied electric field $\boldsymbol{E}$ is described by the induced polarization density $\boldsymbol{P}$, this response can be expanded into [1, 7]

$$P=P^{L}+P^{NL}=\varepsilon_0\chi^{(1)}E+\varepsilon_0\chi^{(2)}EE+\varepsilon_0\chi^{(3)}EEE+... \qquad (\mathbf{1\text{-}1})$$

where $\chi^{(n)}$ is the n^{th} order susceptibility. It is worth noting that the odd-order susceptibilities are present in any material; whereas the even order susceptibilities only exist in noncentrosymmetric materials due to symmetry reasons.

If only the second order term in Equation (1-1) is considered. Assuming the external electric field has a form of

$$E(t)=E_1e^{i\omega_1 t}+E_2e^{i\omega_2 t}+c.c. \qquad (\mathbf{1\text{-}2})$$

the expansion of $\varepsilon_0\,\chi^{(2)}E\cdot E$ will generate frequency components at $2\omega_1$, $2\omega_2$, $(\omega_1+\omega_2)$, and $(\omega_1-\omega_2)$. The first two terms are responsible for second harmonic generation (SHG) and the later two are responsible for summation frequency generation (SFG) and difference-frequency generation (DFG) respectively. If $E_1e^{i\omega_1 t}$ is an optical field and $E_2e^{i\omega_2 t}$ is an applied electric field, the $\chi^{(2)}$ term will then give rise to the Pockels effect (linear E-O effect). Since SHG and Pockels effect are both proportional to $\chi^{(2)}$, in some situation SHG signal can be used to monitor the change in Pockels effect.

A figure from *Introduction to Organic Electronic and Optoelectronic Materials and Devices* [7] describes the relation between the different kinds of 2nd order nonlinear optic effects very clearly.

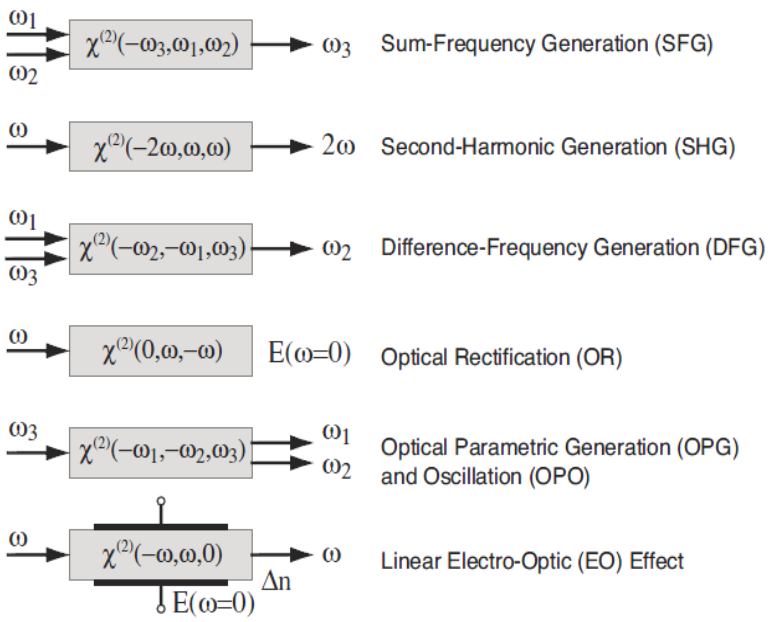

Figure 1-1. Schematic representation of important nonlinear optical effects of the second-order, including the linear electro-optic effect (Pockels Effect).[7] Figure adapted from Ref 7. Copy right CRC textbooks.

When we talk about the E-O activity of an organic material, in most of the cases we are referring to the Pockels effect, which describes the change in birefringence in an optical medium in response to an applied electric field as:

$$\Delta n_i = (-\frac{{n_i}^3}{2}) r_{ij} E_j \qquad \textbf{(1-3)}$$

where n_i is the refractive index in i-direction, E_j is the applied field strength in j-direction, and r_{ij} stands for the tensor component that connects n_i and E_j. Although there do exist other forms of E-O activities, such as electro-absorption, Stark effect, and Kerr effect, in this dissertation, we will confine our discussion of E-O activity to Pockels effect only.

Most amorphous organic E-O materials have C_∞ symmetry in their active form. It can be proved that only the r_{33} and r_{13} (r_{31}) terms are non-zero in the E-O coefficient tensor under this symmetry, where r_{33} is the largest component with r_{33}:r_{13}=3:1. And since the E-O effect originates from the $\chi^{(2)}$ term, the r_{33} can be expressed with $\chi^{(2)}$ as shown in Equation **1- 4**.

$$r_{33} = r_{zzz} = -\frac{2\chi_{zzz}^{(2)}}{n_z^4} \qquad \textbf{(1- 4)}$$

The discussion above has been focused on the bulk properties, while the development of better organic E-O material needs more molecular level understanding. Modern organic E-O materials usually consist of a mixture of an active hyperpolarizable chromophore and an inert matrix. The active chromophore is usually a "push-pull" type charge transfer molecule consisting of an electron-rich donor, a π-conjugated bridge and an electron- deficient acceptor (D-π-A) as shown in **Figure 1-2**.

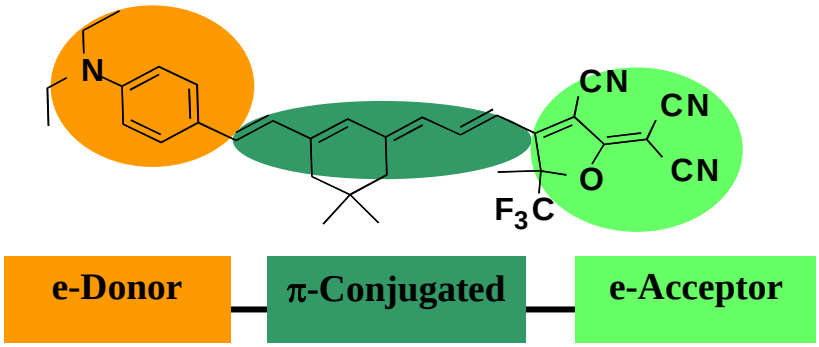

Figure 1-2. Illustration of a typical "push-pull" type D-π-A charge transfer chromophore.

The response of such a molecule to an applied electric field *E* can be described by an induced polarization *p*.

$$p = \alpha E + \beta EE + \gamma EEE + \ldots \qquad \textbf{(1-5)}$$

where α is called the linear polarizability, β is the first order hyperpolarizability and γ is the second order hyperpolarizability. Just like the $\chi^{(2)}$ term in the bulk analysis, here β is responsible for all 2nd order nonlinear optic effects.

To convert the molecular property β into the bulk property $\chi^{(2)}$, parameters describing the amount, angular distribution, and dielectric surrounding of the active molecules must be included. Such a conversion can be written into

$$\begin{aligned}\chi^{(2)}_{//}(\omega_1,\omega_2,\omega_3) &= \chi^{(2)}_{zzz}(\omega_1,\omega_2,\omega_3) = N f_z^{\omega_1} f_z^{\omega_2} f_z^{\omega_3} \left\langle \cos^3\theta \right\rangle \beta_z \\ \chi^{(2)}_{\perp}(\omega_1,\omega_2,\omega_3) &= \chi^{(2)}_{zxx}(\omega_1,\omega_2,\omega_3) = \chi^{(2)}_{zyy}(\omega_1,\omega_2,\omega_3) = N f_z^{\omega_1} f_y^{\omega_2} f_y^{\omega_3} \left\langle \cos\theta \sin^2\theta \right\rangle \beta_z\end{aligned} \qquad \textbf{(1-6)},$$

if we introduce number density *N*, the local field factors *f*s with designated frequencies ($\omega_1, \omega_2, \omega_3$) and directions (***x, y, z***), as well as θ, the angle between the ***z*** axis and the direction of each single molecule. $\langle \quad \rangle$ is the average over every molecule in the system. The presence of $\langle cos^3\theta \rangle$in the equation means that all the chromophores in the bulk need to be oriented or "poled" to give the bulk macroscopic 2nd order nonlinearity. Otherwise in a random system with no preferential orientation, $\langle cos^3\theta \rangle$ is 0.

The relation between bulk r_{33} and molecular properties can thus be derived by combining equation (**1-4**) and (**1-6**) :[2, 7]

$$r_{33} = \frac{-2N(f_z^{\omega})^2 f_z^0 \beta_z \langle cos^3\theta \rangle}{n_z^4} \qquad \textbf{(1-7)},$$

where $\langle cos^3\theta \rangle$ can be estimated according to Boltzmann distribution of non-interacting molecules with dipole moment μ under applied electric field E_p as

$$\langle cos^3\theta \rangle = L_3\left(\frac{\mu\, f_p\, E_p}{k\, T}\right) \quad \textbf{(1-8)},$$

where

$$L_n(x) = \frac{\int_{-1}^{1} cos^n\theta \cdot \exp\left(-xcos\theta\right)\boldsymbol{d}\left(cos\theta\right)}{\int_{-1}^{1} \exp\left(-xcos\theta\right)\boldsymbol{d}\left(cos\theta\right)} \quad \textbf{(1-9)}.$$

It can be estimated that when n=3 and $\frac{\mu\, f_p\, E_p}{k\, T}$ is small,

$$\langle cos^3\theta \rangle = L_3\left(\frac{\mu\, f_p\, E_p}{k\, T}\right) \approx \frac{\mu\, f_p\, E_p}{5\, k\, T} \quad \textbf{(1-10)}$$

Thus

$$r_{33} \approx \frac{-2N(f_z^{\omega})^2 f_z^0 \beta_z}{n_z^4} \cdot \frac{\mu\, f_p\, E_p}{5\, k\, T} \quad \textbf{(1-11)}$$

1.2 Development of organic E-O materials

As has been mentioned previously, the active part of modern organic E-O materials is typically a "push-pull" type charge transfer molecule called chromophore (**Figure 1-2**). These chromophore molecules can either be physically dispersed as a guest component into a passive host or be covalently connected to the host molecule as side-chains or even parts of main chain. Alternatively, dendritic chromophores can form molecular glass type E-O materials by themselves and organic E-O crystals have also been demonstrated as very efficient ways to achieve E-O active bulk material. Since organic E-O crystals have very different properties and

thus design rules from all those amorphous organic E-O materials mentioned above, it is out of the scope of this dissertation, which mainly focuses on the amorphous E-O materials.

The 2nd order nonlinearity of a chromophore is defined by its 1st order hyperpolarizabilityβ. Thus producing larger β is usually considered as the primary molecular level approach to improve the E-O activity. One design rule of large β chromophores is the two-level model, which states that if only one electronic excited state (e) is strongly coupled to the ground-state (g), then β can be expressed by the following expression [8]

$$\beta = \frac{\Delta\mu_{ge}\mu_{ge}^2}{E_{ge}^2} \qquad (\mathbf{1\text{-}12})$$

where $\Delta\mu_{ge}$ is the difference between the excited and ground-state dipole moment, μ_{ge} is the transition dipole moment, and E_{ge} the transition energy. Equation (**1-12**) suggests that there are three direct ways to increase β, (1) enlarging $\Delta\mu_{ge}$, (2) increasing the transition dipole μ_{ge}, and (3) decreasing E_{ge}, which can be characterized by the optical (HOMO-LUMO) bandgap. [2]

In 1994, S. Marder *et al* further suggested to use bond length alternation (BLA, or Δr) as a critical parameter to optimize β. [9-10] Their study showed that the β values of their target molecules were correlated to the BLA as illustrated in **Figure 1-3**. Thus they suggested that there is an optimal combination of donor and acceptor strength for each specific bridge, which can maximize the β value.

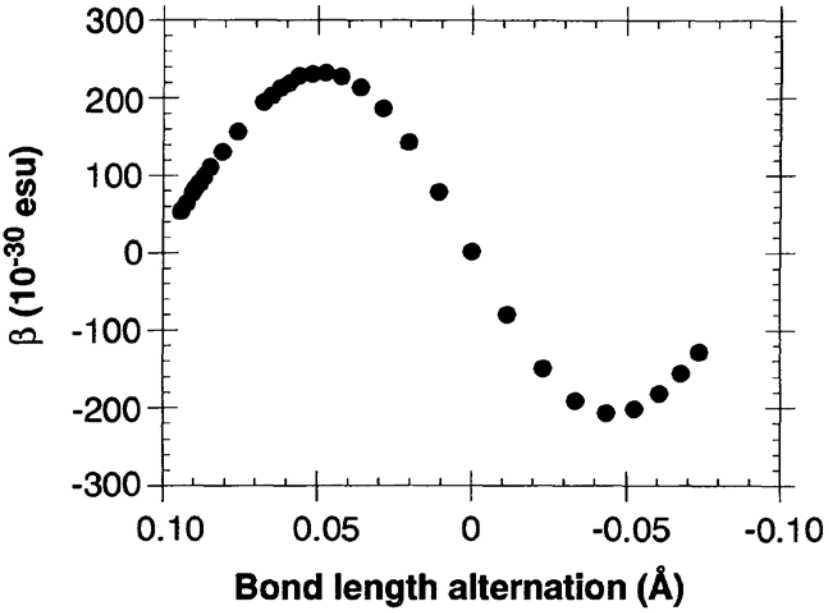

Figure 1-3. Plot of β versus $\langle \Delta r \rangle$, generated with an AM1 geometry optimization (in the MOPAC package) for $(CH_3)_2N$-$(CH{=}CH)_4$-CHO in the presence of a static electric field (generated with point charges) of varying strength. For each value of the static field, and thus $\langle \Delta r \rangle$, β was calculated by a finite-field procedure. [9] Figure adapted from Ref 9. Copy right American Association for the Advancement of Science.

The theories above have been focused on producing larger β, while also worth noting is that Equation (**1-11**) predicts that increasing the loading density N of chromophore can also bring linear enhancement to the E-O coefficient. But in experiments, this "N approach" had encountered a lot of difficulties before the effect of intermolecular electrostatic interactions of chromophores were explained.[2, 5, 11]

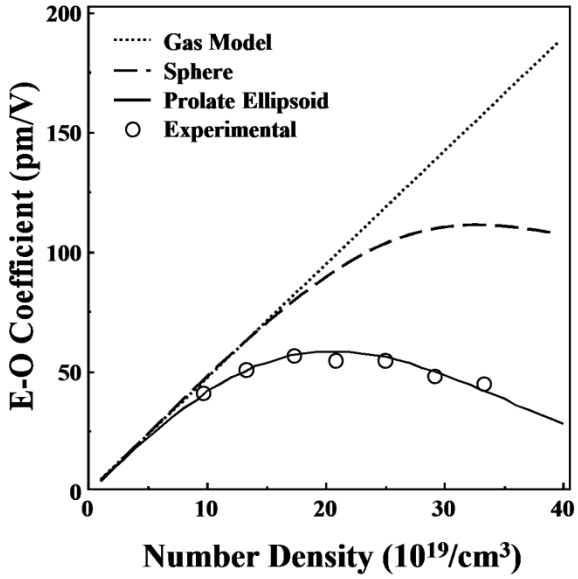

Figure 1-4. Theoretical prediction of E-O coefficients versus chromophore number density of chromophores in different shapes when intermolecular electrostatic interactions are considered. [2] Figure adapted from Ref 2. Copy right *J. Mater. Chem., 1999*

As suggested by Dalton et al, the intermolecular electrostatic interactions have a trend to cancel the alignment under applied external electric field, and this effect gets more pronounced when the loading number density *N* is increased. Thus there exists a maximum loading density *N* for any specific amorphous organic E-O material system, after which further increase in loading will bring negative effect to the overall E-O coefficient. Also, the shape of chromophore plays an important role defining the intermolecular interactions. A spherical shape molecule has more advantage in preventing destructive interaction than “flatter” molecules.

With the guidance of all these theoretical design rules, organic E-O materials have experienced a very fast development in the past 20 years as measured by both the $\mu\beta$ product and r_{33} as shown in **Figure 1-5**.[12]

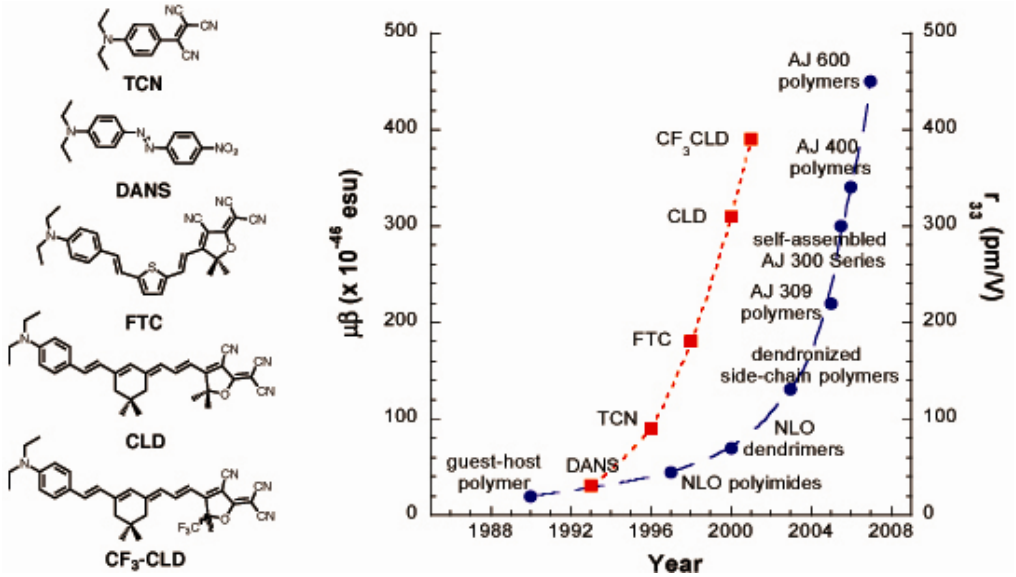

Figure 1-5. The chronological variation of the product of chromophore first hyperpolarizability (β) and dipole moment (μ) is shown in red (dotted line) while the variation of electro-optic activity (r_{33}) is shown in blue (dashed line). [12] Figure adapted from Ref 12. Copy right Polymers 2011.

1.3 Organic E-O materials in photonic applications

Although organic E-O materials have been widely exploited in a lot of photonic applications, modulators are by far the most studied application. E-O modulators are the key components to

transduce electric signal to optical signal, which are essential for telecommunication and high speed optical interconnection.

Mach-Zehnder (M-Z) modulator is a very common design for E-O modulator. As shown in **Figure 1-6**, an M-Z modulator usually has two separated arms. One or both of the arms are poled E-O polymer waveguides. When an electric signal is applied, a phase difference between the two beams will be generated, and the output light intensity, as the interference result of the two arms, can thus be modulated. In modern M-Z modulators using organic E-O material, sub-volt driving voltage and less than 6 dB insertion loss have been achieved separately. [13-15]

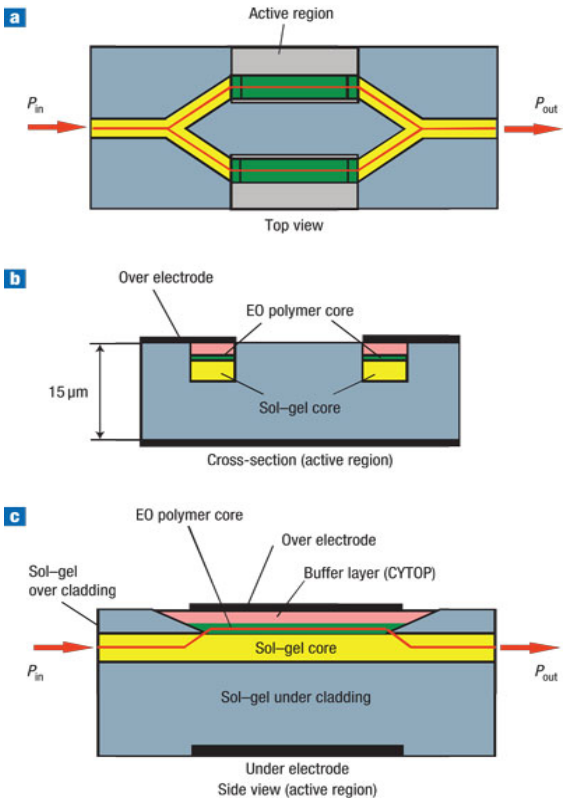

Figure 1-6. The device structure of an M-Z modulator. a) top view of the device; b) cross-section of the active region; c) side view of the active region. [15] Figure adapted from Ref 15. Copy right Nature Photonics 2007.

Ring resonators are another widely used device structure. A ring resonator usually consists of a waveguide in closed loop that is coupled to one or more input/output waveguides. It only propagates wavelengths that satisfy the constructive interference conditions. **Figure 1-7** shows a nano-slot waveguide based ring resonator and its transmission spectrum.[16] If the loop part is made of poled organic E-O material, its transmission peak will be subject to change under applied electric signal. Ring resonators are a good platform to make small footprint, high bandwidth modulators.[17] Ring resonator that operates at 165 GHz has been demonstrated with organic E-O material.[18]

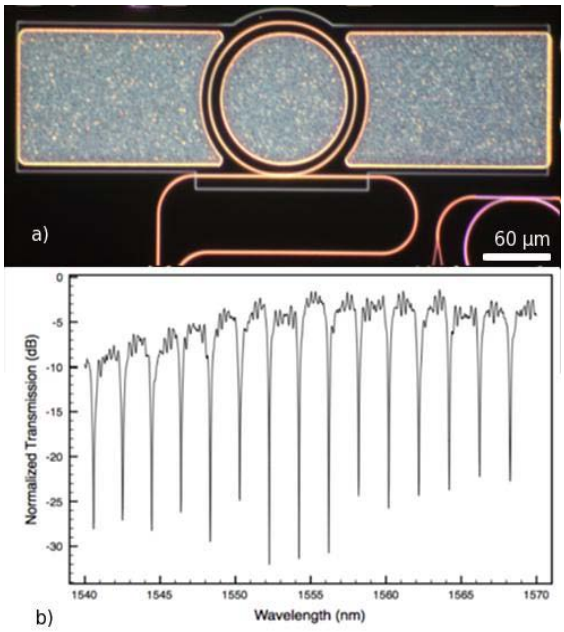

Figure 1-7. (a) Dark field optical micrograph of a nano slot ring resonator; (b) transmission spectrum of the device. [16] Figure adapted from Ref 16 Copy right Opt. Express 2011.

Other than modulators, the research of utilizing organic E-O material to generated THz wave has also attracted a lot of attention. THz is known as the spectral gap between infrared and microwave, which has a frequency range of $0.3\text{-}30\times10^{12}$ Hz. THz waves are promising in applications such as imaging, time domain spectroscopy, and optical-pump/probe spectroscopy. But these applications have been largely limited by the availability of a compact THz source that can provide bright THz wave with a broad and continuous spectrum.

A widely used method to generate THz wave is DFG from 2^{nd} order nonlinear materials. Inorganic 2^{nd} material crystals such as ZnTe have been used for such purpose. The problem of these systems is that due to the phonon absorption of the crystalline material, the emitted THz lacks a smooth frequency response. Amorphous organic E-O materials are good alternatives to avoid such problems. In addition, amorphous organic E-O materials can potentially generate wide THz bandwidth with much higher efficiency.

For all the above mentioned applications, an ideal organic E-O material is expected to simultaneously possess large E-O coefficient (r_{33}), low optical loss, high optical damage threshold as well as excellent alignment temporal stability. Usually these properties cannot be completely settled by synthetic efforts because processing condition also plays an important role defining those parameters, especially for applications with complicated device structures. Without proper processing, even with the best organic EO material the performance of a well-designed real device can be severely compromised. Thus the processing of amorphous organic E-O materials is a very critical research aspect.

1.4 Scope of this dissertation

We have mentioned that amorphous organic E-O materials need to be poled to gain E-O activity. It is this poling process that breaks the centrosymmetric nature of amorphous materials and brings collective orientation to all the chromophores in the bulk and thus non-zero $<cos^3\theta>$. However this aligned state is not energetically stable for most chromophores and is subject to relaxation after the poling field is removed, which can dissipate the E-O activity of the poled material. Thus how to effectively introduce and preserve chromophore orientation are regarded as the primary targets in the processing of organic E-O materials.

$$r_{33} = \frac{-2N(f_z^{\omega})^2 f_z^0 \beta_z \langle cos^3\theta \rangle}{n_z^4} \qquad \textbf{(1-7)}$$

Chapter 2 of this dissertation focuses on a barrier layer approach to improve the poling efficiency of E-O polymers. First of all, high conduction current from excessive charge injection is identified as a fundamental challenge of effective poling. After analyzing the conduction mechanism, we introduce a sol-gel derived thin titanium dioxide (TiO_2) layer that can significantly block excessive charge injection and reduce the leakage current during high field poling. Ultralarge E-O coefficients, up to 160–350 pm/V at 1310 nm have been achieved by poling with such a barrier, which are 26%–40% higher than the results poled without such a TiO_2 layer. This enhancement is explained by a field distribution flattening effect at high injection barrier with the insertion of the TiO_2 barrier layer.

In Chapter 3, the impact of the inserted barrier layer on the temporal alignment stability of E-O polymers is discussed. Considerable stability enhancement is realized using both standard 500-hour temporal alignment stability test at 85 ^oC and thermally stimulated discharge method. We suggest that the enhancement comes from improved stability of the screening charge. During

poling the additional barrier layer helps to lower the injection and thus the space charge accumulation. And this reduced space charge accumulation further helps to replace the space charge part in the total formulation of screening charge with more stable interface trapped charge. We thus expand this knowledge to a group of other materials that can also block excessive charge injection and suppressed space charge accumulation, including dielectric polymers polyvinyl alcohol (PVA), poly(4-vinylphenol) (PVP) and TOPAS as well as ferroelectric polymer poly(vinylidene fluoride-*co*-trifluoroethylene) (P(VDF-TrFE), 65/35 copolymer), which differ largely from the others in dielectric constant, conductivity and surface properties. The only common feature of them is that they all lowered the charge injection and leakage current for 1-2 orders during poling. On every buffer layer we tried, similar trend of stability enhancement is found. These results suggest that the observed temporal stability enhancement is indeed an effect from the abovementioned mechanism.

Chapter 4 focuses on the development of an innovative new poling method, which utilizes pyroelectric effect instead of external power sources to overcome the limitations of conventional contact poling and corona poling. With careful theory assisted design, we developed a reliable protocol to efficiently introduce dipole orientation in organic E-O materials by heating and cooling them with detachable pyroelectric crystals. This new method can potentially improve the process adaptability of organic E-O materials in a variety of photonic devices. Large Pockels coefficients (up to 81 pm/V at 1.3 μm) have been successfully achieved in thin films poled using this method. The effective fields in these experiments are estimated to be around 0.5 to 0.9 MV/cm, which agree well with the electrostatics analysis using an idealized model. The same method is directly applied to surface modified hybrid polymer silicon slot

waveguide ring-resonator modulators devices. A 25 pm/V tunability of resonance peak wavelength shift has been realized, which was higher than any reported results in similar devices.

Chapter 5 discusses about the possible application of the pyroelectric poling in a different device architecture. A long-existing challenge to pole E-O polymer based photonic devices is how to effectively drop the poling voltage to the core layer, which is usually sandwiched between two dielectric claddings. In the past, this was done by using relatively conductive claddings, which on the other hand can bring larger optical loss to the waveguide. Thus careful engineering compromise must be made between better poling efficiency and lower optical loss. Pyroelectric poling as discussed in Chapter 4 opens up new possibilities. In this chapter, it is demonstrated that E-O polymer films can be poled even with 3 orders thicker dielectric layer in circuit using pyroelectric poling. The theoretical analysis matches well with the experimental results. It could provide new insight to the research of poling E-O polymers in hybrid photonic devices, where the E-O materials form intimate contact with different types of materials in the system.

Notes to Chapter 1

[1] D. M. Burland, R. D. Miller, C. A. Walsh, *Chemical Reviews* 1994, **94**, 31.

[2] L. R. Dalton, W. H. Steier, B. H. Robinson, C. Zhang, A. Ren, S. Garner, A. Chen, T. Londergan, L. Irwin, B. Carlson, L. Fifield, G. Phelan, C. Kincaid, J. Amend, A. Jen, *Journal of Materials Chemistry* 1999, **9**, 1905.

[3] M. Hochberg, T. Baehr-Jones, G. Wang, M. Shearn, K. Harvard, J. Luo, B. Chen, Z. Shi, R. Lawson, P. Sullivan, A. K. Y. Jen, L. Dalton, A. Scherer, *Nature Materials* 2006, **5**, 703.

[4] C. V. McLaughlin, L. M. Hayden, B. Polishak, S. Huang, J. D. Luo, T. D. Kim, A. K. Y. Jen, *Applied Physics Letters* 2008, **92**, 151107.

[5] L. R. Dalton, *Journal of Physics: Condensed Matter* 2003, **15**, R897.

[6] L. Dalton, *Polymers for Photonics Applications I, Advances in Polymer Science*, **Vol. 158** (Ed: K.-S. Lee), Springer Berlin / Heidelberg, 2002, 1.

[7] M. J. a. P. Gunter, *Introduction to Organic Electronic and Optoelectronic Materials and Devices*, CRC Press, Boca Raton, Florida 2008.

[8] J. Oudar, *Journal of Chemical Physics* 1977, **66**, 2664.

[9] S. R. Marder, L.-T. Cheng, B. G. Tiemann, A. C. Friedli, M. Blanchard-Desce, J. W. Perry, J. Skindhøj, *Science* 1994, **263**, 511.

[10] G. Bourhill, J.-L. Bredas, L.-T. Cheng, S. R. Marder, F. Meyers, J. W. Perry, B. G. Tiemann, *Journal of the American Chemical Society* 1994, **116**, 2619.

[11] Y. Shi, C. Zhang, H. Zhang, J. H. Bechtel, L. R. Dalton, B. H. Robinson, W. H. Steier, *Science* 2000, **288**, 119.

[12] L. Dalton, S. Benight, *Polymers* 2011, **3**, 1325.

[13] C. T. DeRose, Y. Enami, C. Loychik, R. A. Norwood, D. Mathine, M. Fallahi, N. Peyghambarian, J. D. Luo, A. K.-Y. Jen, M. Kathaperumal, M. Yamamoto, *Applied Physics Letters* 2006, **89**, 131102.

[14] C. T. Derose, R. Himmelhuber, D. Mathine, R. A. Norwood, J. Luo, A. K. Y. Jen, N. Peyghambarian, *Optics Express* 2009, **17**, 3316.

[15] Y. Enami, C. T. Derose, D. Mathine, C. Loychik, C. Greenlee, R. A. Norwood, T. D. Kim, J. Luo, Y. Tian, A. K. Y. Jen, N. Peyghambarian, *Nature Photonics* 2007, **1**, 180.

[16] M. Gould, T. Baehr-Jones, R. Ding, S. Huang, J. Luo, A. K. Y. Jen, J.-M. Fedeli, M. Fournier, M. Hochberg, *Optics Express* 2011, **19**, 3952.

[17] B. A. Block, T. R. Younkin, P. S. Davids, M. R. Reshotko, P. Chang, B. M. Polishak, S. Huang, J. D. Luo, A. K. Y. Jen, *Optics Express* 2008, **16**, 18326.

[18] B. Bartosz, H. Yu-Chueh, T. Hidehisa, S. Byoung-Joon, L. Jingdong, K. Y. J. Alex, H. S. William, R. F. Harold, *Selected Topics in Quantum Electronics*, IEEE Journal of 2007, **13**, 104.

Chapter 2. Enhanced poling efficiency of organic E-O materials using a thin TiO_2-modified transparent electrode

2.1 Background and motivation

As has been discussed in Chapter 1, amorphous organic E-O materials need to be poled to show 2nd order nonlinearity. The commonly used approach to pole such a material is to apply high electric field at a temperature near the glass transition temperature (T_g) of that material in order to orient the dipolar chromophores. In a well designed material system, when the intermolecular interaction between chromophores is negligible, the theoretical E-O coefficient r_{33} is related to the poling electric field by Equation (**1-11**), which implies that r_{33} should be linearly proportional to the poling electric field E_p.

$$r_{33} \approx \frac{-2N(f_z^{\omega})^2 f_z^0 \beta_z}{n_z^4} \cdot \frac{\mu f_p E_p}{5 k T} \qquad (\mathbf{1\text{-}11})$$

In reality, this linear relation holds only when the applied electric field is low. A practical r_{33} *vs.* E_p plot usually looks like Figure 2-1, where at first r_{33} increases linearly with E_p until around $80\text{-}100\ MV/m$ when the curve starts to saturate and then decreases after a maximum is reached. At a certain point, dielectric break down will happen, which could physically destroy the material.

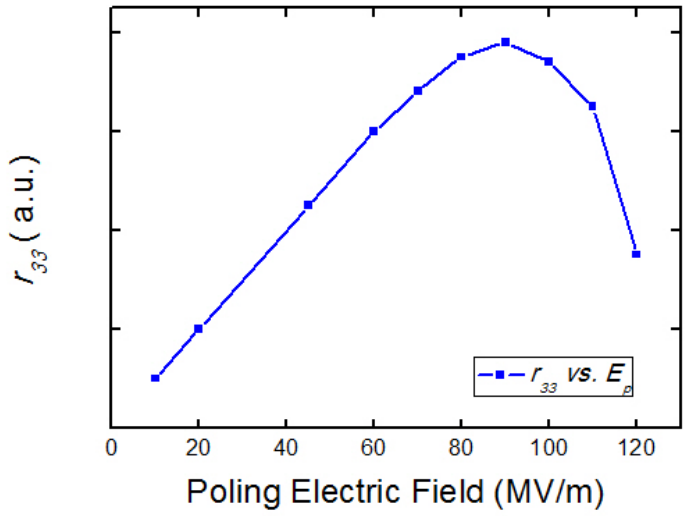

Figure 2-1. Illustration of an r_{33} *vs.* E_p plot of a practical organic E-O material.

The problems come from both the dielectric and electrical properties of the organic E-O materials. First of all, the highest applicable poling electric field is limited by the dielectric strength of the material. Besides the intrinsic electron avalanche breakdown, high leakage current (LC) during poling can lead to electronic-thermal breakdown due to strong local Joule heating, which can significantly lower the dielectric strength of polymers.[1] Secondly, due to the conduction mechanism of E-O polymers, space charge accumulation during poling can destroy the homogeneity of electric field, causing variation of poling efficiency across the E-O material. [2-3] Thus it would be plausible if there is a method to lower the conductivity of E-O polymer during high field poling and increase the dielectric strength at the same time.

One effective approach to improve the poling efficiency is to insert a thin layer of spin-on materials as a barrier between the electrode and the EO layer to form a double-layer structure (**Figure 2-2**).

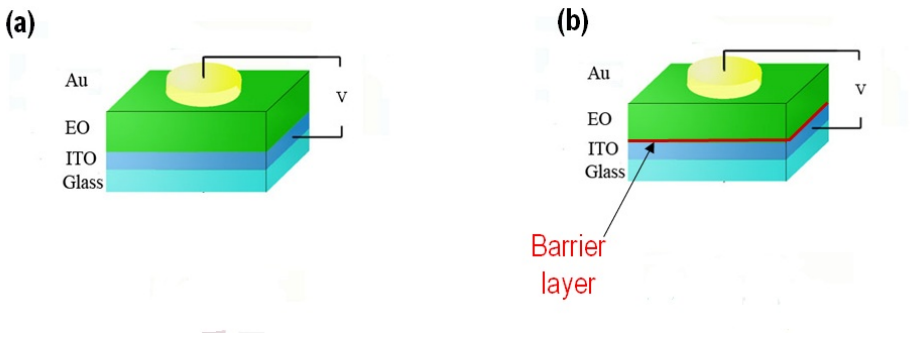

Figure 2-2. Sandwiched (a) single-layer and (b) double-layer structures for the poling of thin film organic EO materials.

By careful selection of the barrier material, this additional layer can effectively block the excessive LC and suppress the onset of catastrophic breakdown to enhance the maximum applicable poling field. Eich *et al* reported the first comprehensive study on high-electric-field poling of sidechain poly(methyl methacrylate-co-DR1 methacrylate) (PMMA/DR1) with a barrier layer.[4-5] They investigated the electrical conduction phenomena during the poling and found that the current densities appeared to be interface (electrode) limited. The electric current and second-harmonic measurements were performed simultaneously to derive the poling efficiency. As shown in **Figure 2-3**, the field dependence of the current density was primarily Schottky emission for medium field strengths (E_{pol} = 100 V/μm), and it was dominated by Fowler-Nordheim tunneling at higher poling fields. By introducing a spin-on inorganic siloxane barrier layer, the tunneling currents were significantly suppressed and the probability of dielectric breakdown was greatly reduced, leading to 20% higher effective internal poling field strength and higher degree of orientational order of poled films.

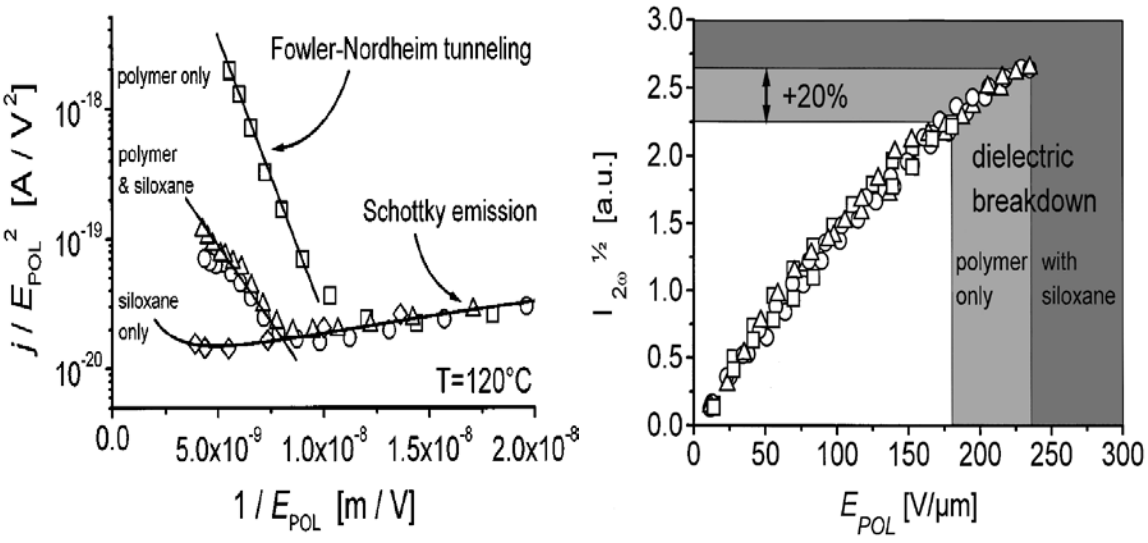

Figure 2-3. **Left**: Fowler–Nordheim diagram, i.e., $ln(j/E^2)$ vs. $1/E$ plot for PMMA/DR1. [squares: polymer only, circles: polymer with 0.13 μm siloxane layer, triangles: polymer with 1.1 μm siloxane layer, diamonds: single inorganic layer]. **Right**: Square root of SHG intensity that is proportional to the achieved degree of chromophore orientation as a function of the applied electric field across the E-O layer defined as $E_{POL} = U_{POL}/d_{TOTAL}$. Figure adapted from ref [4-5]. Copyright 1998 Optical Society of America.

Following the aforementioned study, Drummond *et al* used a conductive-polymer-based cladding layer to enhance the poling in guest-host PMMA/DR1.[6] This study elucidated how the more conductive cladding layer can improve the poling efficiency of multiple layer films. In conventional optical waveguide devices, the active E-O layer is usually sandwiched between two low refractive-index cladding layers that have similar thickness to the active EO layer. During poling, this triple-layer stack can be simply treated as three resistors in series, thus cladding layers with higher conductivity can lead to more effective poling field across the active layer. More recently, researchers have also used the blend of a conducting polymer, poly (ethylene

dioxythiophene) (PEDOT): poly (styrene sulfonate) (PSS) with poly (vinyl alcohol) (PVA) as a conductive cladding layer.[7] An effective poling field of 230 V/μm can be applied on the samples with these clads, whereas the best single-layer EO polymer samples can only sustain 160 V/μm. This led to a 15% enhancement of E-O coefficient over that of the single-layer control sample, which was mainly attributed to the delayed onset of catastrophic breakdown in the double-layer structures.

Grote *et al* have also conducted a thorough analysis of achieving efficient poling and low driven voltage:(V_π) of E-O polymers.[8] Prior to this study, the dielectric constants of both the NLO polymer core, such as PMMA/DR1 and amorphous polycarbonate (APC) doped with CLD1 chromophore, and passive polymer cladding materials used for conventional polymer-based integrated optic devices were very similar in magnitude. This suggests that only a small fraction of the applied modulation voltage can reach the NLO polymer core layer. This contributes to 4-5 times higher modulation voltage than the desired V_π. In Grote's study, a 2-fold decrease in modulation voltage could be achieved by using the conductive polymer PEDOT/PSS, due to its much higher conductivity and dielectric constant than the core material at the modulation frequency.

In summary, previous studies have demonstrated that the application of a suitable barrier layer can improve poling efficiency of the commonly used NLO polymers, such as poly(methyl methacrylate-*co*-Dispersed Red 1 methacrylate) (**PMMA/DR1**), and doped amorphous polycarbonate (**APC**) systems. The r_{33} values of these polymers were enhanced by 15 - 100% compared to those processed with only single-layer active polymer films.

However, the underlying mechanisms regarding the high field poling of NLO polymers remain unclear, especially for the newly developed material systems with much higher concentration of highly nonlinear NLO chromophores. These material systems usually contain high loading density (N of up to $2.5 - 3.5\times10^{20}/cm^3$) of highly polarizable chromophores, and show relatively high conductivities on the order of 10^{-8} - 10^{-11} S/cm during the poling process. At low to medium field strengths (50 - 100 V/μm), the poled single-layer films of these materials exhibited very large r_{33} values of up to 110 - 250 pm/V. Linear extrapolation of such performance to higher poling field indicates that there exists strong potential to achieve unprecedented E-O activity. However, the high poling field often leads to large LC and dielectric breakdown of these materials, which significantly lowers the yield of efficiently poled samples. The high conductivity of these E-O polymers also impose more limitations on selecting suitable materials as the barrier layer that needs to have matched electrical, dielectric, and optical properties for reliable processing and characterization of poled films. Large experimental errors could be encountered in estimating the actual r_{33} values of the E-O core in a sandwiched double-layer structure, where lies the partition of AC voltages between the barrier and E-O layer, as well as the contribution of multiple reflections in highly birefringent films. [9] These problems add extra uncertainties to quantitatively analyze the actual poling efficiency, and its dependence on the average applied field (AAF) and the conduction mechanism of the material systems.

In the following part of Chapter 2, a sol-gel derived TiO_2 thin film was investigated as the barrier layer for poling highly nonlinear E-O polymers. The TiO_2 film, with thickness around 40 nm on top of the ITO substrate, was selected due to its high electrical conductivity, large dielectric constant, and excellent thin film processibility. Such combined properties of the TiO_2 thin film allow the majority of the poling and AC modulation voltages to be applied effectively

across the micron-thick active polymer layer. This greatly simplifies the quantitative correlation between the poling field strength and r_{33} values of the poled films. In the poling study with new E-O polymers containing high concentration of chromophore, the thin TiO_2 barrier layer significantly blocks the excessive charge injection and improves the poling efficiency of materials. As a result, ultralarge r_{33} values (up to 350 pm/V at 1310 nm) have been obtained, which are about 26% to 40% higher than those achieved from poling the single-layer films. This may be due to that the carrier transport across the micron-thick polymer film significantly affects the electric field distribution of the films, and ultimately determines the poling efficiency of these E-O polymers.

2.2 Experimental studies

Titanium (IV) isopropoxide (Aldrich, 99.999%) diluted in *n*-butanol (Aldrich, anhydrous 99.8%) was spin-coated onto low-reflectivity ITO substrates (supplied by Thin Film Devices Inc.) at 3000 rpm. The films were hydrolyzed under ambient condition overnight and then annealed at 450 °C in a vacuum oven for 30 minutes to allow the growth of crystalline anatase TiO_2 films.[10] This protocol typically gives high optical quality TiO_2 layers with thickness around 40 nm and surface roughness of less than 0.5 nm as measured by using atomic force microscope (AFM).

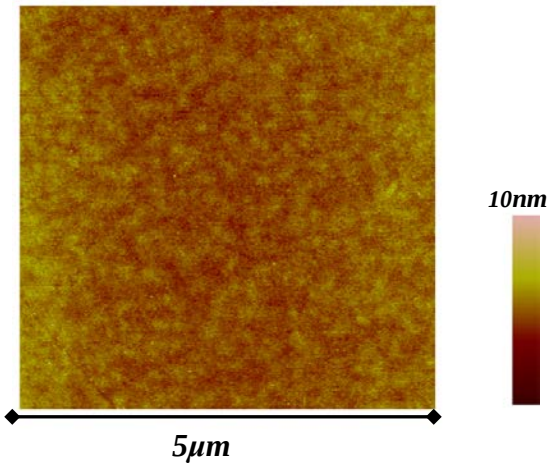

Figure 2-4. AFM image of the TiO_2 modified ITO surface.

The E-O materials used in this work were **AJ-CKL1**, **AJ307**, and **AJ404** (**Figure 2-5**). **AJ-CKL1** is a guest-host polymer in amorphous polycarbonate (**APC)** doped with 30 wt% of chromophore **1**. **AJ307** is a guest-host polymer in polymer **3** with 25 wt% of chromophore **2**. The host polymer **3** is a high-T_g polymer with good optical properties and has excellent compatibility with dipolar chromophores. **AJ404** is a new E-O polymer containing binary chromophore systems.[11] All these polymer systems contain relatively high chromophore loading (N ~ 3.0 - $3.5\times10^{20}/cm^3$). The solutions of these polymers in 1,1,2-trichloroethane or cyclopentanone were first filtrated through 0.2-μm syringe filter, then spin-coated onto both TiO_2-coated ITO and bare ITO substrates, respectively. The films were baked in a vacuum oven at 80 °C for 10 h, and the film thickness was measured to be around 1.2 - 1.8 μm. The gold electrode was sputtered on top of the polymer films for contact poling and for the measurement of E-O coefficients.

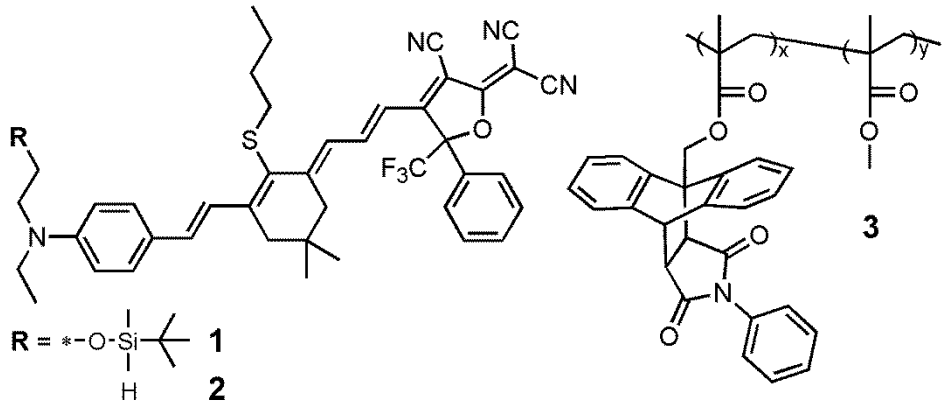

Figure 2-5. Chemical structures of chromophores and host polymer used in this study.

Through a four-probe measurement, the conductivity of the prepared TiO_2 layer was found to be around 1.5×10^{-4} S/cm, which is four orders higher than the peak conductivity of the E-O polymer. The dielectric constant of TiO_2 films through similar processing has been reported to be ~ 42 at 1 kHz,[12] which can be further enhanced by thermal annealing. Given these parameters, it can be determined that the voltages for poling and modulation could be applied nearly completely across the layer of E-O core.[8]

To pole the films, the field was set at 100 - 125 V/μm at the initial temperature of 50 °C. The LC during poling was monitored with a Keithley 617 electrometer. The samples were heated at a constant ramp rate of 10 °C/min to the glass transition temperature (T_g) of polymers, at which a rapid increasing in LC was often observed. The poled samples were then cooled to ambient temperature. After removal of the applied field, the r_{33} values of poled films were measured by using the Teng-Man reflection technique at the wavelength of 1310 nm, and the values were calibrated after taking into account the effects of multiple-reflection.[9, 13]

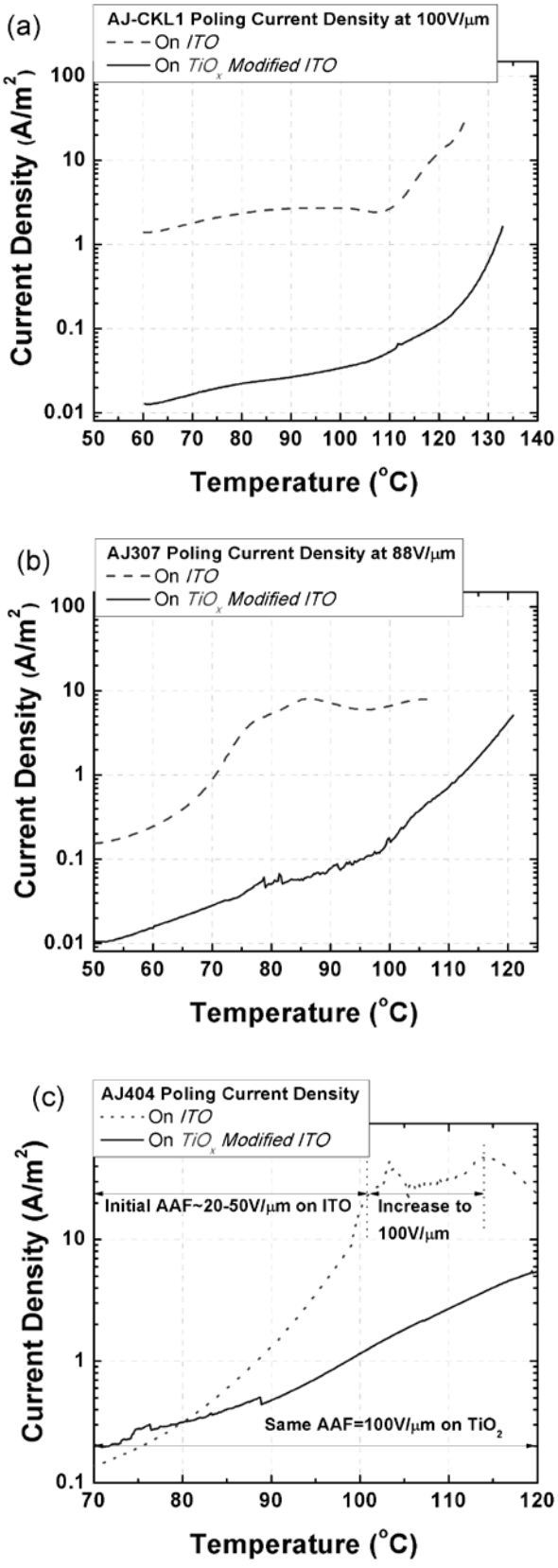

Figure 2-6. Current density versus temperature plots for (a) **AJ-CKL1** polymer at AAF=100V/μm; (b) **AJ307** polymer at AAF=88V/μm and (c) **AJ404** at condition specified in figure.

It can be seen that the insertion of the TiO_2 barrier significantly reduces the density of LC by one to two orders of magnitude (**Figure 2-6**). This can be explained by the fact that the TiO_2 layer is an excellent barrier to block excessive hole injection due to its low lying valence band (~7.4 eV).[14] With the TiO_2 barrier, the maximum achievable r_{33} values of these polymers can be enhanced substantially to ~ 40% higher for both **AJ-CKL1** and **AJ404** and 26% higher for **AJ307** as compared to their single-layer values, respectively.

Table 2-I. Summary of the poling results of AJ-CKL1, AJ307, and AJ404

	ITO		***TiO_2-coated ITO***		*Overall*
	Best r_{33} values (pm/V)	*r_{33}/AAF ($(nm/V)^2$)*	*Best r_{33} values (pm/V)*	*r_{33}/AAF ($(nm/V)^2$)*	*improvement in optimal r_{33} values*
AJ-CKL1	112	1.12	156	1.25	39%
AJ307	133	1.33	168	1.68	26%
AJ404	250	2.50	350	3.50	40%

The efficiency of dipole alignment in these poled films was quantified by a series of comparative experiments (**Table 2-I**). Under the same poling field, higher r_{33} values could be achieved. Plots of r_{33}-AAF show a significant increase in slope by inserting the TiO_2 barrier film compared to the single-layer devices. In **AJ-CKL1**, the r_{33}-AAF slope increases by 11% and the rest of the r_{33} enhancement due to the elevated poling field. In **AJ307** and **AJ404**, the r_{33} improvements are mainly from the steeper r_{33}-AAF slope, which are enhanced by 26% and 40%, respectively. Such enhancement has not been reported from prior studies, in which the higher r_{33} values of poled films were mainly due to the increased poling field while the r_{33}-AAF slopes

were nearly unchanged. At a given field, the r_{33}-AAF slope can only be altered by the effective field distribution across the material, which in turn is related to the conduction mechanism of E-O polymers.

Therefore, the current-voltage (*J-V*) response of E-O polymers has been further investigated. Arkhipov *et al* have used a unified model to study hopping of the injected charge carriers and the space charge limited current (SCLC) to simulate the current behavior and field distribution of disordered organic materials.[15] This model considers the conduction as a combined result from a two-step injection and a hopping SCLC in organic materials with a Gaussian density of states distribution. The temperature, field, and thickness dependences of injection limited current (ILC) and SCLC have been also quantitatively described.[15-17] In molecularly doped polymers, such dependence arises naturally from the interaction of charge carriers with randomly distributed permanent dipoles.[18] In this study, a strong electric field around 10^6 V/cm is applied to micron-thick films of E-O polymers. We expected that the poling efficiency of E-O polymers is determined by the interplay between ILC and SCLC under different conditions.

To verify this assumption, we have measured the *J-V* response of the **AJ-CKL1** films with and without the TiO_2 barrier at different temperatures. As shown in **Figure 2-7 (a)**, the proposed model from Arkhipov fits well with our experimental results.[15] Such a good agreement indicates that the analytic model of SCLC and ILC can be applicable to the poling of E-O polymers, and their current behavior and field distribution under high poling field can be more quantitatively estimated. In **Figure 2-7 (b)**, the spatial distribution of electric field across the films was shown. Since the sandwiched single-layer film has relatively low injection barrier at the ITO/polymer

interface, excessive holes can be injected into the E-O polymers and the SCLC determines the *I-V* characteristics. Consequently, quite inhomogeneous field distribution exists during poling. On the contrary, due to the very low HOMO level of TiO_2, the injection barrier has been dramatically enhanced by nearly 3.0 eV at the modified ITO/polymer interface, causing sufficient suppression of the hole injection. Therefore, the dominant conduction mechanism in this device configuration is injection limited,[16] and the distribution of poling field remains almost constant.

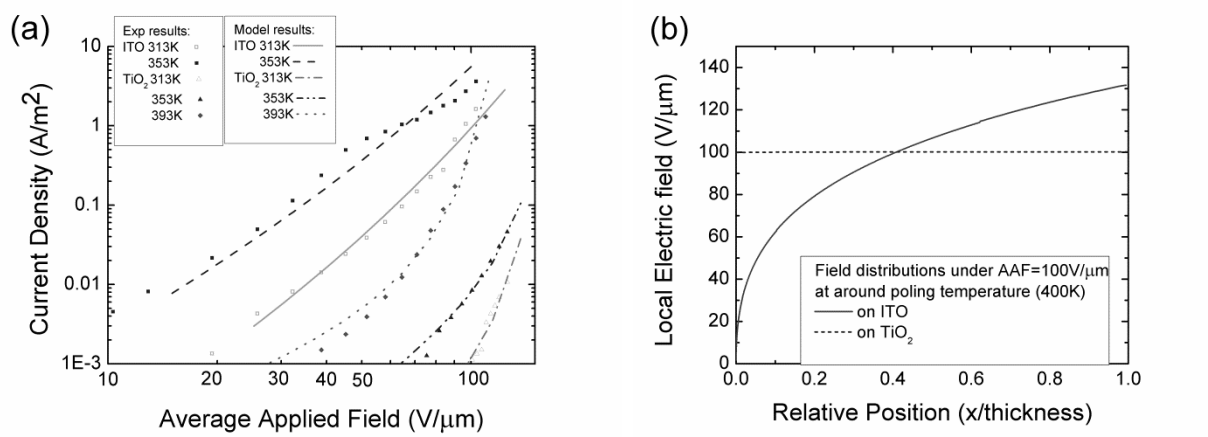

Figure 2-7. (a) **AJ-CKL1** *J-F* response with/without TiO_2 layer at different temperatures. The dots are experiment results and the lines are from calculation. (b) Using the same parameter from (a), the field distributions are calculated in a normalized scale.

2.3 Conclusion

The poling efficiency of high chromophore concentration E-O polymers in this study is known to be very sensitive to both temperature and the actual applied field strength. We conceived that it was the degree of field bending effect that determines the poling efficiency of E-O polymers at different poling conditions. Without the TiO_2 barrier layer, an uneven field distribution led to inhomogeneous poling of E-O films, and the partial discharge occurs at the end with higher field strength, even under an averaged critical voltage lower than the breakdown voltage of the whole system. Furthermore, a nonuniform electric field could act as the dielectrophoretic force, and draw more polarized particles from the weak field to the intense field region.[19] This can cause micro-phase separation and high poling-induced optical loss.[20] It could also impede the efficient poling of materials, due to the fact that relatively high loading density of chromophores is close to the saturation point of these guest-host polymers. It should be mentioned that the bending in electric field distribution due to SCLC has been reported frequently in other areas of organic semiconductors. [15-18, 21-22] However, prior to this study, it has not been applied to the poling study of E-O polymers.

In conclusion, we have demonstrated a spin-on TiO_2 layer that can significantly improve the poling efficiency of highly nonlinear polymer systems of **AJ-CKL1**, **AJ307** and **AJ404**. The present work differs from previous efforts in the following aspects. It applied a unified model of SCLC and ILC, which has been used in the study of molecular semiconductor devices, to explain the current behavior and field distribution of poled polymers. It identified the field distribution flattening effects as the major factor in enhancing the poling efficiency of E-O polymers. This effect can be achieved by selecting suitable materials, such as the sol-gel derived TiO_2 as the barrier layer. Due to its low lying valence band, the TiO_2 layer can effectively block hole

injection from the anode, and keep injection as the rate-controlling factor during poling. This allows the poling process to be performed with lower LC and more homogeneous field distribution, which leads to higher efficiency (enhancement of 26% − 40%) in these highly efficient E-O polymers.

Notes to Chapter 2

[1] M. Ieda, *IEEE Transactions on Electrical Insulation* 1980, **EI-15**, 206.

[2] S. Huang, T. D. Kim, J. D. Luo, S. K. Hau, Z. W. Shi, X. H. Zhou, H. L. Yip, A. K. Y. Jen, *Applied Physics Letters* 2010, **96,** 243311.

[3] J. Luo, S. Huang, Z. Shi, B. M. Polishak, X.-H. Zhou, A. K. Y. Jen, *Chemistry of Materials* 2010, **23**, 544.

[4] M. Sprave, R. Blum, M. Eich, *Applied Physics Letters*, 1996, **69**, 2962.

[5] R. Blum, M. Sprave, J. Sablotny, M. Eich, *Journal of the Optical Society of America B* 1998, **15**, 318.

[6] J. P. Drummond, S. J. Clarson, J. S. Zetts, F. K. Hopkins, S. J. Caracci, *Applied Physics Letters* 1999, **74**, 368.

[7] C. T. DeRose, Y. Enami, C. Loychik, R. A. Norwood, D. Mathine, M. Fallahi, N. Peyghambarian, J. D. Luo, A. K.-Y. Jen, M. Kathaperumal, M. Yamamoto, *Applied Physics Letters* 2006, **89**, 131102.

[8] J. G. Grote, J. S. Zetts, R. L. Nelson, F. K. Hopkins, L. R. Dalton, C. Zhang, W. H. Steier, *Optical Engineering* 2001, **40**, 2464.

[9] D. H. Park, C. H. Lee, W. N. Herman, *Optics Express* 2006, **14**, 8866.

[10] S. K. Hau, H.-L. Yip, O. Acton, N. S. Baek, H. Ma, A. K. Y. Jen, *Journal of Materials Chemistry* 2008, **18**, 5113.

[11] T.-D. Kim, J. Luo, Y.-J. Cheng, Z. Shi, S. Hau, S.-H. Jang, X.-H. Zhou, Y. Tian, B. Polishak, S. Huang, H. Ma, L. R. Dalton, A. K. Y. Jen, *The Journal of Physical Chemistry C* 2008, **112**, 8091.

[12] A. K. Hassan, et al., *Journal of Physics D: Applied Physics* 2003, **36**, 1120.

[13] C. C. Teng, H. T. Man, *Applied Physics Letters* 1990, **56**, 1734.

[14] M. Gratzel, *Nature* 2001, **414**, 338.

[15] V. I. Arkhipov, H. V. Seggern, E. V. Emelianova, *Applied Physics Letters* 2003, **83**, 5074.

[16] P. M. Borsenberger, L. Pautmeier, H. Bassler, *The Journal of Chemical Physics* 1991, **94**, 5447.

[17] R. Agrawal, P. Kumar, S. Ghosh, A. K. Mahapatro, *Applied Physics Letters* 2008, **93**, 073311.

[18] D. H. Dunlap, P. E. Parris, V. M. Kenkre, *Physical Review Letters* 1996, **77**, 542.

[19] K. C. Kao, *Dielectric Phenomena in Solids*, Elsevier Academic Press, San Diego 2004.

[20] C. C. Teng, M. A. Mortazavi, G. K. Boudoughian, *Applied Physics Letters* 1995, **66**, 667.

[21] P. W. M. Blom, M. J. M. de Jong, M. G. van Munster, *Physical Review B* 1997, **55**, R656.

[22] F. Michelotti, *Journal of Applied Physics* 1998, **83**, 7886.

Chapter 3. Enhanced temporal stability of a highly efficient guest-host electro-optic polymer through barrier layer assisted poling process

3.1 Background and motivation

For any potential photonic application, alignment temporal stability is another highly desired property for an ideal organic E-O material candidate. As has been discussed in the introduction part, the poled state of amorphous organic E-O material is not energetically stable for most chromophores and is subject to relaxation. This relaxation can dissipate the alignment ($<cos^3\theta>$) and thus the E-O activity (r_{33}) of the poled material. To keep stable operation of any photonic device, it is of primary importance to minimize this relaxation after the poling field is removed. Researchers have demonstrated enhanced temporal stability by covalent incorporation of E-O chromophores into main-chain or side-chain polymers, introducing crosslinking mechanism[1-4], molecular self-assembly[5] or using physical anchoring effect between chromophores and the polymer matrix [6]. Although all these approaches have certain degree of success, they often involve extra synthetic efforts and delicate processing protocols. It would be advantageous if a generally applicable method can be developed to improve the temporal stability of E-O polymers without engaging the abovementioned complex processes.

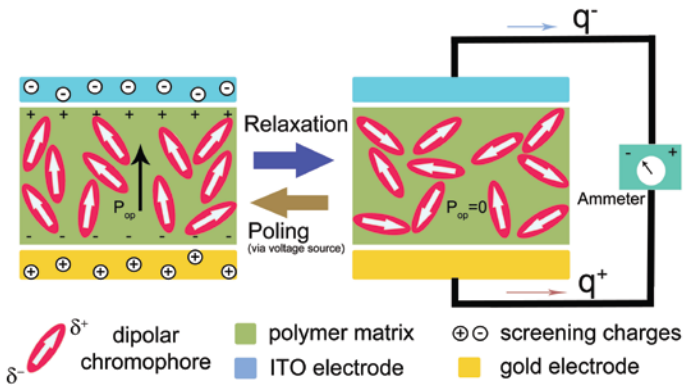

Figure 3-1 When a poled E-O polymer film is subject to relaxation, the screening charges that originally compensated the orientational polarization are gradually released following the decrease in orientational polarization.

Here in this chapter, we provide new systematic study on how the basic properties of E-O polymers as dipolar polymer electrets can significantly affect their temporal stability at elevated temperatures. With sufficiently high field strength around 100 V/μm, the poling process of E-O polymers can create a large orientational polarization (P_{op}) of the molecular dipoles. After poling, like typical polymer electrets, the P_{op} needs to be compensated by some screening mechanisms at places where the P_{op} is not constant, especially near two polar surfaces of polymer films, to reach equilibrium. Thus the negative and positive screening charges are respectively formed at two polar surfaces of poled films, and attracted by the oriented molecular dipoles. During relaxation, as the poling-induced polar orientation gradually decays, the P_{op} diminishes accordingly with the release of screening charges. This process can be recorded as thermally stimulated discharge current (TSD), which is performed by connecting two electrodes of a poled E-O polymer film to an ammeter while heating the film at a constant rate to accelerate the relaxation (**Figure 3-1**).

Previously the TSD technique has been widely used to study the relaxation dynamics of polymer electrets (including second-order nonlinear optical polymers) as a function of temperature.[7]

Of our particular interest is the electret effect of newly developed high performance E-O polymers that contain high concentration of large hyperpolarizability (β) chromophores. These material systems contain high loading density (N of up to 2.5-3.5×10^{20}/cm3) of tetraene chromophores with strong dialkylaminophenyl donors and CF3-TCF acceptors. Due to very large dipole moment (μ) of chromophores, expectedly the Pop of their poled films could be stabilized by the enhanced forces of dipole/screening-charge attraction and head-to-tail dipole-dipole interaction. However, experimentally demonstration of such stabilization mechanism has not been successful for new generation E-O polymers, and very little is known about the possibility of using screening process as a secondary factor to affect the temporal stability of E-O polymers.

A distinct feature of these high efficiency E-O polymers is high leakage currents (LC) during the poling process, and the LC peak with conduction current density greater than 10 A/m2 corresponds to high DC conductivities around 10^{-8}-10^{-11} S/cm for their single-layer poled films that are sandwiched between two electrodes. This level of conductivity is several orders higher than that of early generation of E-O polymers such as PMMA-DR1 and other polymer electrets. Consequently, a large portion of the screening process to the formed P_{op} is developed by the injected charges, which accumulate near the positive electrode as space charge region. After poling, these space charges tend to dissipate through diffusion or recombination and can be gradually disintegrated from their original binding with P_{op}, triggering a relaxation pathway of poled E-O films that is relatively independent of the molecular relaxation mechanisms for bulk

materials. We speculate that the space charge effect be one of major factors in screening process that limits the temporal stability of poled films.

To test the above hypothesis, we select the sol-gel derived TiO_2 as a barrier layer to modify the indium-tin-oxide substrate. Due to its low lying valence band (7.4 eV), the TiO2 layer is known to be a very effective barrier to dramatically reduce the hole-injection and suppressing the space charge accumulation during the poling process, leading to improved poling efficiency of E-O polymers.[8] Our focus in the chapter is to see if the barrier layer approach can create more stable and localized screening charges through the suppression of space charge accumulation, thereby affecting the temporal stability of poled E-O films. Besides the sol-gel derived TiO_2, the selection of barrier layer materials also include a series of dielectric polymers, such as polyvinyl alcohol (PVA), poly(4-vinylphenol) (PVP), cyclic olefin copolymer (TOPAS) and the ferroelectric polymer poly(vinylidene fluoridetrifluoroethylene) (P(VDF-TrFE), 65/35 copolymer). All these materials differ largely from each other in dielectric constants, conductivities and surface properties, and studying their potential effects on the temporal stability of poled E-O films can contribute to improved understanding of E-O polymers as amorphous dipolar polymer electrets. In addition, it could provide ample insight to the research of E-O polymers for hybrid photonic platforms, where the E-O materials form intimate contact with different types of materials in the system, such as passive dielectric clads, semiconductors and metal electrodes.

3.2 Experimental studies

The TiO_2 barrier layer was fabricated on ITO as reported before.[8] The resulting TiO_2 layer had a thickness of 40 nm and a mean surface roughness of ~0.5 nm as measured by AFM. The E-O polymer used in this study was a guest-host system formulated by doping 35 wt% of a dipolar phenyltetraene chromophore AJLZ53 into amorphous polycarbonate (APC). The AJLZ53 chromophore is a newly developed highly efficient and photo-chemically stable dipolar nonlinear optical (NLO) chromophore based on perturbational molecular orbital theory of Dewar's rule. It can be doped into APC at relatively high loading level. The polymer composite has a T_g around 140 °C, and exhibited exceptional combination of large EO activity, low optical loss and good temporal stability. The dibromomethane solution of this polymer was first filtrated through a 0.2 μm syringe filter and then spin-coated onto ITO substrates with and without TiO_2 barrier layer. The films were baked in a vacuum oven at 80 ^oC for 10 hours to remove the residual solvents. The resulting E-O polymer layer has a thickness of 1-2 μm.

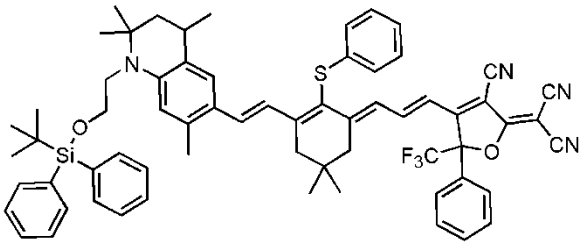

Figure 3-2. Molecular structure of dipolar chromophore AJLZ53.

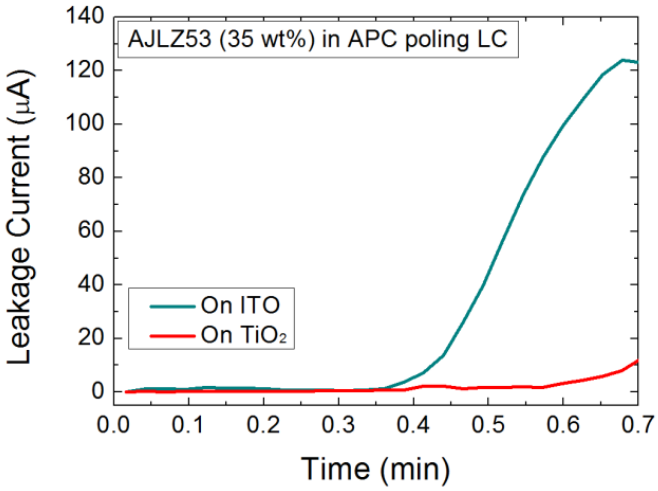

Figure 3-3. Poling LC of AJLZ53 (35 wt%)/APC on ITO substrates with and without TiO_2 barrier**.**

Samples on both TiO_2 modified ITO and unmodified ITO were poled under a unified condition by applying 100V/μm electric field under 140 ^{o}C for 0.7 minute and then fast cooled down to room temperature with the electric field on. During the poling, LC was monitored by a Keithley 617 electrometer and recorded by a computer program. It can be seen that without barrier modification, the peak LC was larger than 100 μA, while on TiO_2 modified substrate the LC was about 10 μA. (see **Figure 3-3**) This was consistent with our previous study that the TiO_2 barrier can prevent the excessive charge injection.

The r_{33} of each poled sample was then measured by the Teng-Man reflection technique at 1310 nm.[9] The resulting r_{33}'s after multi-reflection correction were ~140 pm/V on ITO and ~160 pm/V on TiO_2. [10] 500-hour temporal alignment stability tests were performed on freshly poled

samples at 85°C by measuring the r_{33} change over time. The results were then normalized to their initial r_{33} values for each sample respectively.

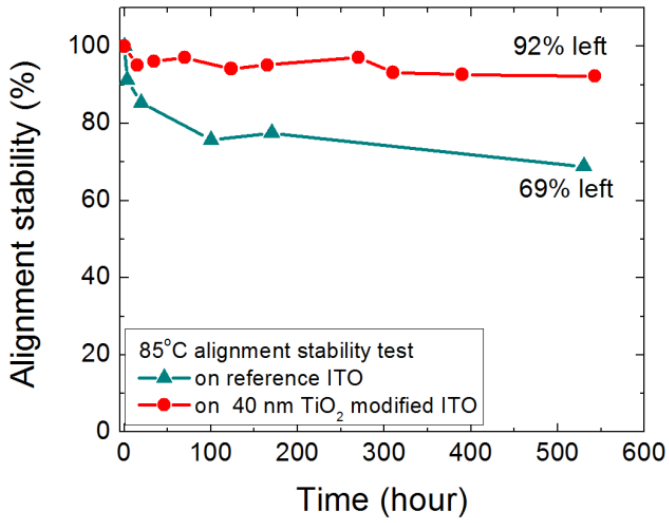

Figure 3-4. 85 °C 500-hour temporal alignment stability results measured on ITO with and without TiO_2 barrier layer.

As shown in **Figure 3-4,** on ITO substrate with no barrier modification, the r_{33} dropped to 69% of its initial value after 500 hours following a Kohlrausch-Williams-Watts (KWW) type decay line,[11] while the TiO_2 modified sample showed a enhanced stability of 92%.

To further understand the underlying mechanism for this enhanced alignment stability, a series of thermally stimulated discharge (TSD) studies were performed.[7] The TSD spectra are displayed in **Figure 3-5**. The relaxation of dipole orientation is responsible for the visible ***α*** peaks at around 125 °C in both spectra.[7,11,12] However this ***α*** peak shifted to 130 °C and became sharper for the poled film with the TiO_2 barrier, as compared to 124 °C when the poled film was only on ITO. On the other hand, it can be directly observed that between 50 and 100 °C the ITO-

only sample showed a notably larger discharge current, which was dominated by the space charge background at this temperature range. This suggests that there were more space charges accumulated in shallow traps in the poled samples with the ITO-only electrode, which can be easily released upon heating or such kind of perturbation. It is also worth to point out that the increasing slope of the curve after this $\boldsymbol{\alpha}$ peak is due to a partially hidden $\boldsymbol{\rho}$ peak, which is also related to the release of charges, but from much deeper traps. The spectra after 150 °C are not shown because after 150 °C the spectra are irrelevant to the alignment relaxation but from more sophisticated morphological and compositional changes of the films.

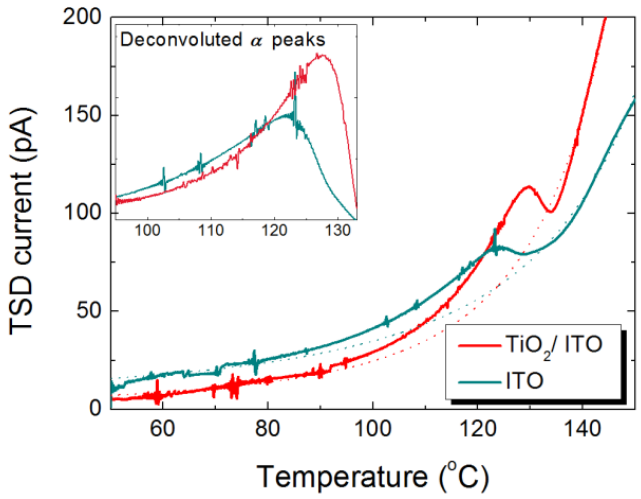

Figure 3-5. TSD spectra of poled AJLZ53/APC films on ITO with and without the TiO_2 barrier layer. Inset shows the deconvoluted α peaks.

Assuming the TSD spectra only consist of an α peak and a ρ peak, we deconvoluted the spectra to calculate the simple Debye type activation energy for the dipole relaxation in each case respectively. This simple model describes the relaxation during a constant-rate TSD as

$$j(T) = dP(T)/dt = -\alpha(T)P(T) \qquad \textbf{(3-1)}$$

$$\alpha(T) = \alpha 0\ exp(-E/kT) \qquad \textbf{(3-2)}$$

where j is the TSD current density, $P(T)$ is the total polarization remaining at temperature T, α is the relaxation rate and E the activation energy.[12] Using standard method, the activation energy for alignment relaxation was estimated to be $143\ kJ/mol$ on TiO_2/ITO and $87\ kJ/mol$ on ITO respectively, indicating a much stabilized alignment on TiO_2. It is worth mentioning that the simple Debye model doesn't consider the distribution of either the activation energy or the natural frequency α, the abovementioned numbers are only qualitatively meaningful.

From these above experimental results, we suggest that the stability enhancement of this TiO_2 barrier layer mainly came from the reduced charge injection from the ITO anode during poling. The low charge injection helped to replace the space charge part in the total formulation of screening charge with more stable interface trapped charge. But other possibilities also exist at this point. For example, the high surface energy of TiO_2[13-14] could have interacted with the oriented polar chromophores to maintain their alignment, or the high dielectric constant of this barrier layer[13] could have somehow helped stabilizing the alignment, and so forth.

To confirm this stabilization mechanism is mainly from the limited injection, while not from any other specific property of TiO_2 itself, it is better to have a comparison with a variety of barriers that can also limit charge injection but have very different other properties. We thus expanded these experiments to a group of materials that can also block excessive charge injection and suppressed space charge accumulation, including dielectric polymers polyvinyl alcohol (PVA), poly(4-vinylphenol) (PVP) and TOPAS$^{@}$ as well as ferroelectric polymer

poly(vinylidene fluoride-*co*-trifluoroethylene) (P(VDF-TrFE), 65/35 copolymer), which differ largely from each other in dielectric constant, conductivity and surface properties. The only common feature of them is that they all can lower the charge injection.

The polymer barrier layers were prepared by spin-coating the corresponding solutions on ITO respectively, followed by a baking process, which completely removed the solvents. The thickness of the different barrier layers was measured with a Dektak 3030 profilometer. Processing information regarding the polymer barrier layers can be found in **Table 3-I**.

Table 3-I. Process parameters of the polymer barrier layers

	Solution	**Spin-rate (rpm)**	**Baking Temperature (^{o}C)**	**Thickness (nm)**
PVA	3 wt% in Hot H_2O	1000	100	120
PVP	5 wt% in isopropyl alcohol	3000	100	400
TOPAS	5 wt% in chlorobenzene	8000	110	200
P(VDF-TrFE)	5 wt% in cyclopentanone	5000	120	100

Poling and stability tests were performed as described before. The LC's during poling are plotted in **Figure 3-6** and the 85 ^{o}C 500-hour temporal alignment stability results in **Figure 3-7**.

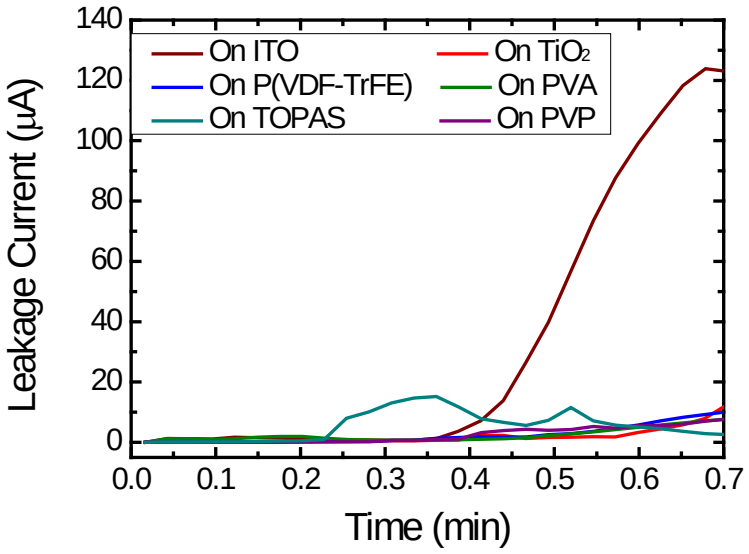

Figure 3-6. Poling LC of AJLZ53 (35wt%)/APC on differently modified substrates**.**

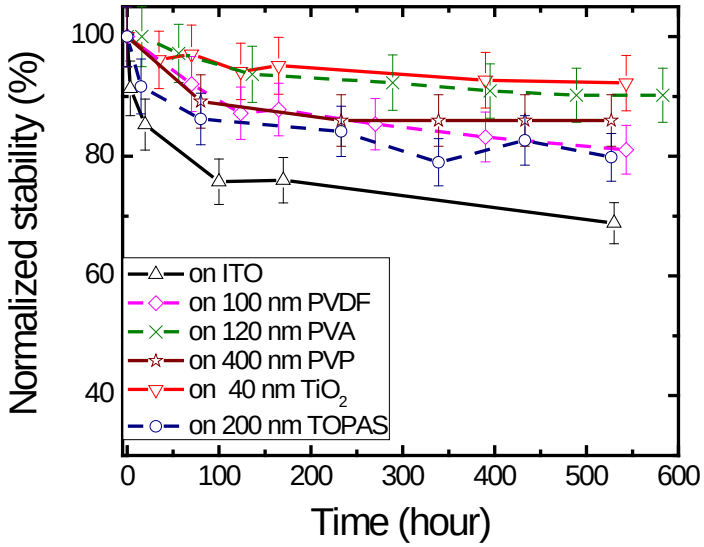

Figure 3-7. 85 ^{o}C 500-hour temporal alignment stability results measured on ITO with and without barrier layers.

It can be seen that on all barrier modified substrates, the poling LC's were in a range of 10-20 μA, which was about an order lower than that on unmodified ITO. This matches our expectation that these barriers can prevent the excessive charge injection. And indeed, we saw stability enhancement ranging from 10% to 21% on all these new barriers. The strongest enhancement is from PVA, which remained 90% of the initial r_{33} after 500 hours under 85 ^{o}C. The lowest enhancement is from the 200 nm TOPAS$^{@}$ polymer barrier, which also maintained about 80% of the original r_{33}. This lower enhancement could be related to those relatively high LC bumps during poling, which may eventually come from the structural features of the TOPAS$^{@}$ polymer. In the case of P(VDF-TrFE), the 500h stability is 81%. Because the stability test was performed at 85 ^{o}C, which was close to the phase transition of P(VDF-TrFE) at 80-100^{o}C [14], this stability result may have been undermined considerably.

Table 3-II. Selected properties of the different barriers compared with ITO.

	Thichness (nm)	**Surface energy** (mJ/m^2)	**Dielectric constant**	**Relative conductivity**	**500h stability** (%)
TiO_2	40	>400 [13-14]	42 [15]	Wide band semiconductor	92
PVA	120	45 [17]	8 [17-18]	Insulator	90
PVP	400	35 [17]	3.9 [17]	Insulator	86
P(VDF-TrFE)	100	51 [19]	~10 [20-21]	Insulator	81
TOPAS$^{@}$	200	31 [22]	~6.7 [23]	Insulator	80
ITO	--	69.2 [24]	--	Good conductor	69

The different properties of all these different materials are summarized in **Table 3-II**. It can be seen that no clear trend in any single listed property alone or their direct combination can determine the effect of temporal alignment stability enhancement.

3.3 Conclusion

In summary, we have systematically compared the temporal alignment stability of poled E-O polymer on ITO substrates with and without a barrier layer. The temporal stability of the poled sample can be significantly enhanced by 23% if a TiO_2 barrier layer is applied. The results from TSD studies confirmed that this stability enhancement is associated with a lowered space charge background, which help improve stability of the screening process. The temporal stability study has also been expanded to cover a variety of polymer-based barrier layers, which have quite different properties. Similar trend of stability enhancement for poling and temporal stability was observed for all polymeric barriers we tested, including PVA, PVP, P(VDF-TrFE) and TOPAS, which provided very convincing data for our hypothesis. These results provide valuable insights for understanding poled E-O polymers in multi-layered structures, which are used in many integrated photonic devices.

Notes to Chapter 3

[1] M. Haller, J. Luo, H. Li, T.-D. Kim, Y. Liao, B. H. Robinson, L. R. Dalton, A. K. Y. Jen, *Macromolecules* 2004, **37**, 688.

[2] Z. W. Shi, J. D. Luo, S. Huang, X. H. Zhou, T. D. Kim, Y. J. Cheng, B. M. Polishak, T. R. Younkin, B. A. Block, A. K. Y. Jen, *Chemistry of Materials* 2008, **20**, 6372.

[3] Z. W. Shi, J. D. Luo, S. Huang, Y. J. Cheng, T. D. Kim, B. M. Polishak, X. H. Zhou, Y. Q. Tian, S. H. Jang, D. B. Knorr, R. M. Overney, T. R. Younkin, A. K. Y. Jen, *Macromolecules* 2009, **42**, 2438.

[4] Z. W. Shi, W. Liang, J. D. Luo, S. Huang, B. M. Polishak, X. S. Li, T. R. Younkin, B. A. Block, A. K. Y. Jen, *Chemistry of Materials* 2010, **22**, 5601.

[5] T.-D. Kim, J.-W. Kang, J. Luo, S.-H. Jang, J.-W. Ka, N. Tucker, J. B. Benedict, L. R. Dalton, T. Gray, R. M. Overney, D. H. Park, W. N. Herman, A. K. Y. Jen, *Journal of the American Chemical Society* 2007, **129**, 488.

[6] B. M. Polishak, S. Huang, J. D. Luo, Z. W. Shi, X. H. Zhou, A. Hsu, A. K. Y. Jen, *Macromolecules* 2011, **44**, 1261.

[7] W. Köhler, D. R. Robello, P. T. Dao, C. S. Willand and D. J. Williams, *Journal of Chemical Physics*, 1990, **93**, 9157.

[8] S. Huang, T. D. Kim, J. D. Luo, S. K. Hau, Z. W. Shi, X. H. Zhou, H. L. Yip, A. K. Y. Jen, *Applied Physics Letters* 2010, **96**, 243311.

[9] C. C. Teng, H. T. Man, *Applied Physics Letters* 1990, **56**, 1734.

[10] D. H. Park, C. H. Lee, W. N. Herman, *Optics Express* 2006, **14**, 8866.

[11] D. M. Burland, R. D. Miller, C. A. Walsh, *Chemical Review* 1994, **94**, 31.

[12] G. Sessler, *Topics in Applied Physics* 1987, **33**, 13.

[13] A. Navrotsky, *Geochemical Transactions* 2003, **4**, 34.

[14] H. Zhang, J. F. Banfield, *Journal of Material Chemistry* 1998, **8**, 2073.

[15] A. K. Hassan, N. B. Chaure, A, K. Ray, A. V. Nabok and S. Habesch, *Journal of Physics D: Applied Physics*, 2003, **36**, 1120.

[16] A. V. Bune, V. M. Fridkin, S. Ducharme, L. M. Blinov, S. P. Palto, A. V. Sorokin, S. G. Yudin, A. Zlatkin, *Nature* 1998, **391**, 874.

[17] T. B. Singh, F. Meghdadi, S. Günes, N. Marjanovic, G. Horowitz, P. Lang, S. Bauer, N. S. Sariciftci, *Advanced Materials* 2005, **17**, 2315.

[18] X. Peng, G. Horowitz, D. Fichou, and F. Garnier, *Applied Physics Letters* 1990, **57**, 2013.

[19] S. Wi, N. Senthilkumar, S. W. Rhee, *Journal of Materials Science-Materials in Electronics* 2008, **19**, 45.

[20] V. Bharti, Q. M. Zhang, *Physical Review B* 2001, **63**, 184103.

[21] Z. M. Dang, Y. H. Lin, C. W. Nan, *Advanced Materials* 2003, **15**, 1625.

[22] P. Munzert, U. Schulz, N. Kaiser, *Surface and Coating Technology*, 2003, **174-175**, 1048.

[23] R. D. Shannon, R. A. Oswald, G. R. Rossman, *Physics and Chemistry of Minerals* 1992, 19, 166.

[24] J. S. Kim, J. H. Park, J. H. Lee, J. Jo, D. Y. Kim, and K. Cho, *Applied Physics Letters* 2007, **91**, 112111.

Chapter 4. Efficient poling of electro-optic polymers by pyroelectric effect

4.1 Background and motivation

As has been discussed earlier, E-O polymers have to be poled to show E-O activity. Usually this is done by applying high electric field at the glass transition temperature (T_g) of that polymer using either contact poling or corona poling. In contact poling, the electric field is applied using highly conductive electrodes that directly connect the E-O film and the external high voltage source.[1-2] (**Figure 4-1**) Whereas in corona poling, the electric field is usually built up upon the charge accumulation on the surface of the EO polymer film, which is under the corona discharge of a sharp needle, wire, or grid charged to several kilovolts.[3-4] (**Figure 4-2**) Although these two protocols are relatively well established, there do exist some challenging problems in both of them. In contact poling, severe charge injection from metal electrodes often results in large leakage current that causes dielectric damage to the material.[1-2, 5] Whereas in corona poling, it is difficult to control the homogeneity and magnitude of the poling field because it critically depends on the corona discharge of the ambient atmosphere. In addition, it tends to create surface damage on the poled films due to various reactive and energetic species from the corona discharge, such as ozone or nitrogen oxides.[6] These problems can strongly inhibit the efficient poling of E-O polymers, especially when photonic devices with complicated geometry are involved.[7-9]

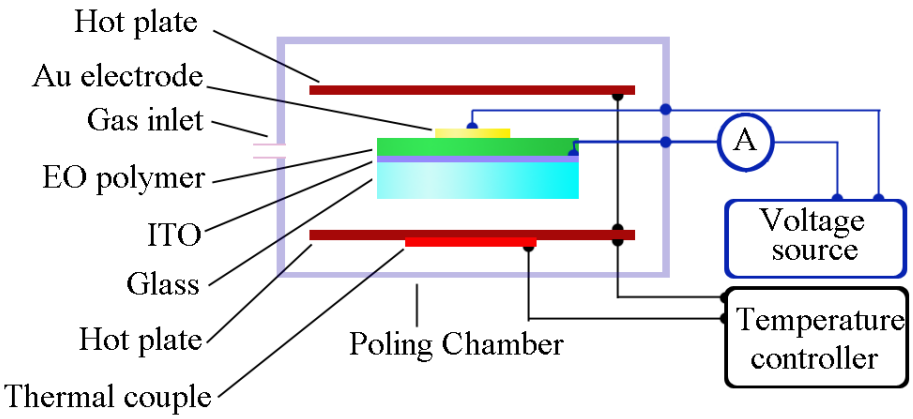

Figure 4-1. Contact poling configuration for organic and polymeric EO materials.

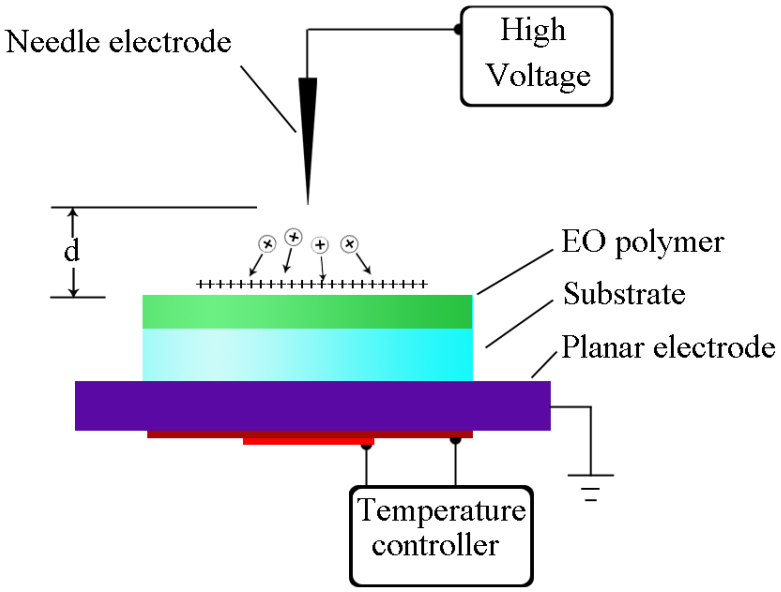

Figure 4-2. Corona poling configuration for organic and polymeric EO materials.

Pyroelectric crystals, which can generate high electric field on their insulating surfaces during temperature change, offer a potential solution to these problems.[10] Pyroelectric crystals,

such as lithium niobate (LN) and lithium tantalate (LT), are crystal materials with an intrinsic spontaneous polarization (P_s). Under the equilibrium condition, this P_s of a pyroelectric crystal is completely balanced by the surface screening charges (σ_{sc}). Heating or cooling of this crystal develop equal but opposite charges on both polar surfaces due to the change of P_s as a function of temperature. However, only a small fraction of these charges exists as free carriers,[11] and the relaxation time of pyroelectric charges can be adjusted by modifying the dielectric structures of the system. The past decade has witnessed a rapid growth in the research of utilizing the electric field generated by pyroelectrics in a variety of applications. The switchable and patternable surfaces of pyroelectric crystals and epitaxial films have been demonstrated as exceptional platforms to study the polarization-dependent surface chemistry of polar molecules,[12-14] the phase transition of material [15] and the wettability of liquid matters.[16] On the other hand, thermally stimulated field emission from pyroelectric crystals, which can create high-energy (>100 keV) charged particles, has been demonstrated as cheap and compact resources of x-rays, electrons, ions, and neutrons.[17-19] When E-O polymers are used as the recipient medium of this depolarization electric field at a suitable temperature, collective orientation of dipolar chromophores is expected. When this poling method is used, we can expect very low charge injection, a uniform poled area that only depends on the size of the crystal, as well as much improved processibility in device applications. Several field-dependent parameters, such as poling-induced E-O activity (r_{33}) and order parameter (Φ) can be quantitatively measured to help understand the electrostatics in pyroelectric systems.

4.2 Theoretical analysis of the electrostatics in pyroelectric poling

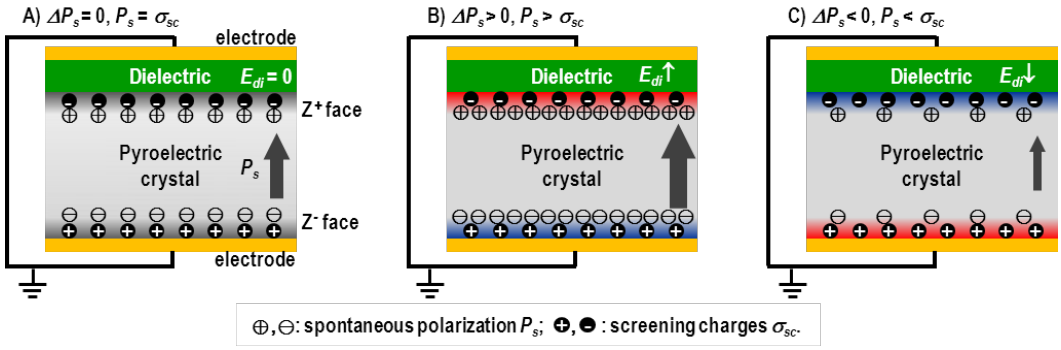

Figure 4-3. Schematic illustration of pyroelectric poling. The bilayer laminate comprises a pyroelectric crystal and a dielectric film (such as E-O polymer) on the Z^+ face surface of the crystal. The large closed arrows in the layer of pyroelectric crystal denote the spontaneous polarization (P_s) of pyroelectric crystals, and the thickness and length of the arrows indicate relative magnitude of P_s at different temperatures. The generation of uncompensated charges (ΔP_s) through the pyroelectric effect is the source of electric field (E_{di}) in the dielectric thin film, and the small open arrows at the thin layer of dielectrics represent the direction of electric fields. Not to scale.

Figure 4-3 shows the schematic drawing of a bilayer laminate comprising a pyroelectric crystal and a dielectric film, where the dielectric film is deposited onto the Z^+ face surface of the crystal. This system can be considered as two capacitors in parallel, and the dielectric film is the recipient medium of pyroelectric field.[10, 20-21] Under the equilibrium condition (**Figure 4-3A**), the bulk P_s is fully compensated by the surface σ_{sc}, therefore there is no electric field everywhere within the dielectric stack. However, when the temperature is varied, it will cause a change of the spontaneous polarization (ΔP_s). This change can be described as $\Delta P_s = \gamma \Delta T$, where γ is the

pyroelectric coefficient of the crystal and ΔT is the change of temperature. When the temperature change is much faster than the charge compensation, an uncompensated net charges density of ΔP_s will stay on the surface in the form of either excessive polarization charges (**Figure 4-3B**) or screening charges (**Figure 4-3C**) before the compensation occurs. These "static" charges are the origin of the depolarization electric field (E_{di}) inside the dielectric medium. If the loss of pyroelectric charges is small, it would yield

$$E_{di} = \gamma \Delta T / [\varepsilon_0(\varepsilon_{di} + \varepsilon_{cr} L_{di}/L_{cr})] \qquad (4\text{-}1)$$

where ε_0, ε_{cr}, and ε_{di} are the dielectric permittivities of free space, the pyroelectric crystal and the dielectric film, respectively. L_{cr} and L_{di} are the thickness of the crystal along the polar axis and the dielectric film, respectively.

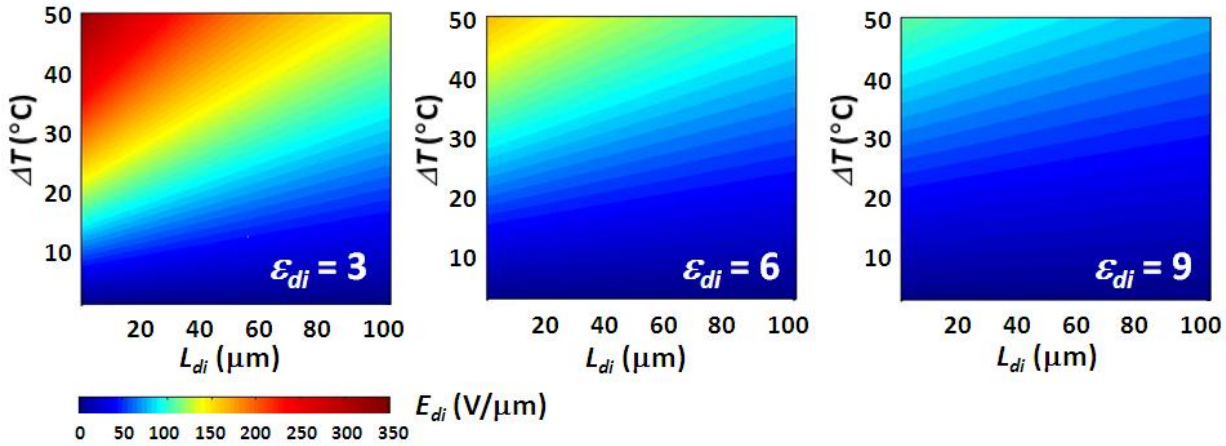

Figure 4-4. Electric field generation (E_{di}) in pyroelectric poling as a function of temperature change (ΔT), thickness (L_{di}), and dielectric constant (ε_{di}) of thin film dielectric materials. The Z-cut lithium tantalate (LT) is selected as the pyroelectric crystal

with a thickness (L_{cr}) of 1.0 mm, γ of 176 μC/(m^2·°C) and ε_{cr} of 43 with respect to equation (**4-1**).

In this idealized model, a modest temperature change (10 °C to 50 °C) in a LT crystal [22] will lead to a considerably large electrostatic field in a thin film dielectric material (**Figure 4-4**). If the ε_{di} of a typical amorphous organic thin film dielectrics is assumed to be 3, the maximum achievable potential on the charged surface can be as high as 15 kV, and the effective field strength in the dielectric films can vary from 50 to 350 V/μm over a broad range of thickness (from sub-micron to 100 μm). This level of static electric field is adequate to align the dipoles of the NLO chromophores or polarize other dielectric materials.

To verify the validity of this idealized model, several physical parameters used in the experiments need to be considered. The leakage of pyroelectric charges through both the crystal and dielectric medium can cause exponential decay of the generated electric fields at the ratio of $exp[-t/(R_{eq}C_{eq})]$, where t is the time in second, R_{eq} is the equivalent resistance in ohms ($R_{eq}^{-1} = R_{cr}^{-1} + R_{di}^{-1}$), and C_{eq} is the total capacitance in farads ($C_{eq} = C_{cr} + C_{di}$) of the system, respectively. R_{cr} and R_{di} are the resistance, and C_{cr} and C_{di} are the capacitance of the crystal and dielectric layer, respectively. In previous studies, when the recipient medium has low permittivity and high resistivity (such as gaseous molecules under high vacuum), the values of $R_{eq}C_{eq}$ are approximate to $R_{cr}C_{cr}$, which gives the relaxation time of greater than 10^5 sec due to very high resistivity (on the order of 10^{15} Ω·m) of LN and LT crystals. Therefore, the leakage due to the bulk conductivities of these systems could be negligibly small over a relatively long time.[11, 20]

However, for amorphous π-functional materials such as E-O polymers and organic semiconductors with resistivity on the order of 10^9 Ω·m or less, the values of $R_{eq}C_{eq}$ are nearly equal to those of $R_{di}C_{di}$ and the relaxation time will drop dramatically to around 10^{-2} sec. This indicates that the majority (> 90%) of the static field from equation (**4-1**) would vanish within 0.1 sec. This analysis underscores the fundamental challenge of pyroelectric poling of E-O polymers, where the relatively low resistivity of E-O polymers provides a pathway for rapid leakage of pyroelectric charges. To solve these problems, we have carefully designed heterogeneous dielectric structures suitable for the poling experiments.

4.3 Experimental studies with E-O polymer thin films

A guest-host polymer was selected for this investigation. Its linear optical and E-O properties of contact-poled films were established as a reference. The measured results of E-O coefficient (r_{33} values), maximum absorbance, and refractive index of the contact-poled films clearly showed their dependence on the poling field strength. This provides a reliable comparison with pyroelectrically poled results. The guest-host polymer was formulated by doping 15 wt% of a dipolar phenyltetraene chromophore **AJLZ53** into poly(methyl methacrylate) (PMMA). The UV-*vis*-NIR absorption spectra of its thin films shows a characteristic π–π* charge-transfer absorption with the absorption maxima (λ_{max}) at 820 nm. This polymer composite has a glass transition temperature (T_g) of 110 °C.

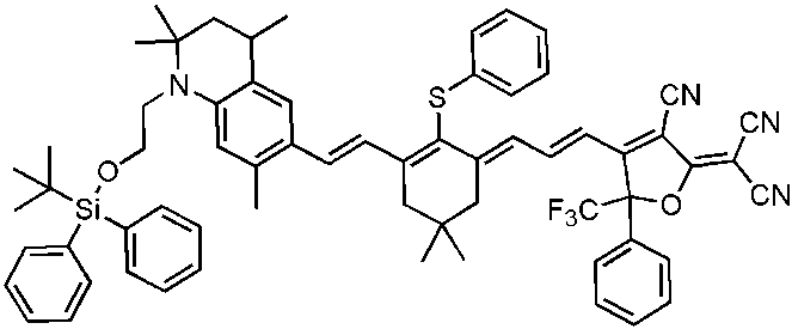

Figure 4-5. Molecular structure of dipolar chromophore AJLZ53.

The dibromomethane solution of this polymer was first filtrated through a 0.2 mm syringe filter and then spin-coated onto ITO substrates with or without barrier layer modification. The films were baked in a vacuum oven at 80 ^{o}C for 10 hours to remove the residual solvents. A thin layer of gold electrode was then sputtered on top of the films, and contact poling were performed at the polymer's glass transition temperature (T_g ~ 110 °C) with a series of electric field (E_{pol}) up to 100 V/μm respectively. The resistivity of the films under this poling condition is around 1.3×10^{9} Ω·m. The r_{33} values of 100 V/μm poled films were ~90 pm/V at the wavelength of 1.31 μm measured by using the Teng–Man reflection technique.[23-24] The r_{33} values were found to be linearly proportional to the E_{pol} at a constant r_{33}/E_{pol} ratio of 0.90 nm^2/V^2, which agreed well with the oriented gas model commonly used for poled polymers.[3]

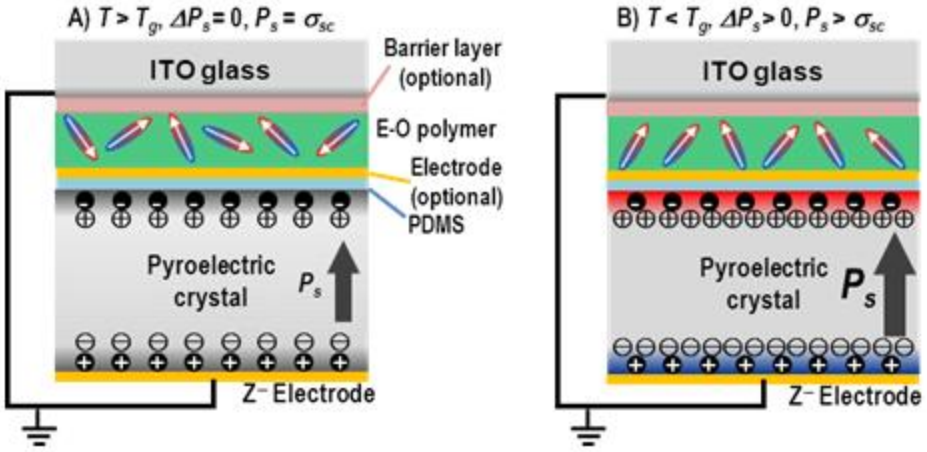

Figure 4-6. The schematic drawings of multi-layered structures for pyroelectric poling of guest-host E-O polymers in the parallel-plate (transverse) design: A) unpoled films; B) poled films. The ellipses in the layer of E-O polymer represent the chromophores with the arrows directed along the chromophoric dipole moments. Note that the PDMS buffer layer provides the soft contact lamination for poling, and the poled films can be lifted off from the crystal for linear optical and E-O measurements. Not to scale.

The efficiency of pyroelectric poling of this standardized E-O polymer critically depends on: 1) the air-gap-free contact between the E-O polymer film and crystal, 2) the balanced thermal profile to provide sufficient temperature change (ΔT) for generating static electric field and orientating dipolar chromophores, and 3) the optimized dielectric structures to prevent or limit the discharge pathways. Among numerous protocols used, a multi-layered structure that can enable very efficient pyroelectric poling of polymers is shown in **Figure 4-6**. In this case, a thin layer (200 nm to 400 nm) of spin-on material, such as poly(vinylidene fluoride-*co*-trifluoroethylene) copolymer (P(VDF-TrFE), 65/35 copolymer) or poly(4-vinylphenol) (PVP) is inserted between ITO electrode and E-O polymer (1.5-3.5 μm thick) as a barrier.

Optical grade Z-cut LT and LN crystals (size, 15mm×15mm; height, 1.0mm) were used in this study. The Z^+ axis is defined as the direction of out-of-the-Z-surface that becomes positive upon cooling. To have a better lamination between the E-O polymer films and the crystal, an ultra-thin layer of polydimethylsiloxane (PDMS) precursor was spin-coated onto both E-O polymer film and the Z^+ surface of LT (or LN) crystal. After cured at 70 °C for 3 hours, a 70 nm soft PDMS elastomer layer was formed on the surface of both the E-O film and the crystal. To perform pyroelectric poling, the crystal flake was brought to the central area of E-O polymer film on ITO slides (size, 25.4mm×25.4mm). An air-free contact formed naturally across the sample. The Z^- surface and ITO electrode were grounded to complete the pre-poling preparation of samples.

Such a soft lamination has been proved very efficient for pyroelectric poling. In addition, after poling the polymer film and the crystal flake can be separated from each other with a razor blade and a pair of tweezers. This protocol provides great convenience for the follow-up characterization.

After the above preparation, the samples were inserted into a digitally controlled hot stage, heated to around 120 °C and held there for 10 minutes. The 10-minute annealing step was to allow the screening charge and spontaneous polarization (P_s) of LT or LN crystal to reach a new equilibrium at elevated temperatures. Then the heating power was turned off and the hot stage was opened, exposing the whole system to the nitrogen atmosphere at ambient temperature. During the temperature change from 120 °C to 100 °C, the pyroelectric field was expected to orient the chromophore dipoles in the polymer. This cooling protocol was able to provide large ΔT, and thus generate a steady and strong electric field for poling the E-O polymer.

After the samples were cooled to room temperature, the crystal flake was removed. The residual PDMS on E-O films was also erased with Q tip and isopropyl alcohol, leaving the stand-alone poled E-O films ready for r_{33} and order parameter characterization. As before, the r_{33}'s of these poled **AJLZ53**/PMMA films were measured by Teng-Man reflection technique.[24-25]

The refractive indices and thicknesses of E-O films were measured by a Metricon 2010 prism coupler. The UV-*vis*-NIR absorption of the poled polymer films were taken on a Perkin-Elmer Lambda 9 spectrophotometer. The spectra of poled films were measured after removing the gold electrodes by KI/I_2 gold etchant. These films were then annealed at 110 °C for 5 minutes, which completely de-poled the sample. And these annealed films were re-measured to give the spectra of unpoled films for comparison. Furthermore, the order parameter of these poled films, defined as $\Phi=\langle(3\cos^2\theta-1)/2\rangle$ was calculated from the obtained absorption spectra of poled films before and after annealing following $\Phi = 1 - A/A_0$, where A and A_0 are the integral of absorbance under the resonance peak for the poled and annealed films at normal incidence respectively.[3-4]

The glass transition temperature of the E-O polymer was determined to be 110 ^oC by analysis of differential scanning calorimeter (DSC), which was conducted in a sealed pan by a TA instruments DSC 2010 with a heating rate of 10 °C/min under the nitrogen atmosphere.

The voltage drop to the stack of **AJLZ53**/PMMA was difficult to measure directly because any external measurement circuit would act as an extra leakage pathway to affect the screening of *in-situ* generated pyroelectric charges (on the level of 0.1 $\mu C/cm^2$). But this voltage can be theoretically estimated (E_{theo}) using equation (**4-1**) if we consider the PDMS/E-O polymer/barrier triple-layer structure as three capacitors linked in series. The change in temperature is defined as $\Delta T = \Delta T_{max} - 100$, where ΔT_{max} is the highest applied temperature. The temperature of 100 °C is

selected as the lowest limit since below this point, further orientational response of chromophores to the pyroelectric field was minimal at the time scale of processing. With the ΔT varied between 20 and 30 °C, the E_{theo} of pyroelectric poling was 75 – 124 $V/\mu m$ for LT and 35 – 58 $V/\mu m$ for LN, respectively. On the other hand, the equivalent field drop across the polymer films during pyroelectric poling (E_{equiv}) can also be estimated from their r_{33} values using the approximated r_{33}/E_{pol} ratio of 0.9 nm^2/V^2, which was experimentally obtained from contact-poled samples. The use of this simple and quantitative approach can avoid complicated local-field corrections.

Table 4-I. Summary of pyroelectric poling for the E-O polymer AJLZ53/PMMA

Sample Entries [a]	**Barrier Layer (thickness)**	**Crystal**	**ΔT (°C)** [b]	**r_{33} (pm/V)** [d]	**E_{equiv} (V/μm)** [f]	**Φ** [e]	**E_{theo} (V/μm)** [c]	**E_{equiv} / E_{theo} (×100%)**
1	PVP (200nm)	LT	15	**60**	67	0.058	75	**89%**
2	PVP (200nm)	LT	20	**81**	90	0.085	99	**91%**
3	PVP (200nm)	LT	25	**78**	87	0.074	124	**70%**
4	P(VDF-TrFE) (360nm)	LT	15	**58**	64	-	75	**85%**
5	P(VDF-TrFE) (360nm)	LT	20	**78**	87	0.076	99	**88%**
6	None	LT	15-25	**6**	6.7	-	75-124	**<8%**
7	PVP (200nm)	LN	20	**42**	47	0.030	47	**100%**
8	None	LN	15-25	**0**	0	N/A	35-59	**0%**

[*a*] Sample configuration is illustrated in **Figure 4-6**; [*b*] $\Delta T = \Delta T_{max} - 100$, where ΔT_{max} is the highest applied temperature, and 100 is selected as the lowest limit; [*c*] E_{theo} is calculated by the derived electrostatic analysis from equation 1, parameters being used for LT: L_{cr} of 1.0 mm, γ of 176 μC/(m^2·°C) and ε_{cr} of 43; and for LN: L_{cr} of 1.0 mm, γ of 83 μC/(m^2·°C) and ε_{cr} of 28 [16]; [*d*] r_{33} values are measured by Teng-Man reflection at 1.3 μm, and V_{eo} is the portion of the total modulation voltage (V_{mod}) that drops across the E-O polymer. It is corrected by the model of two capacitors in series, $V_{eo} = V_{mod}\varepsilon_{bl}/(\varepsilon_{bl}+\varepsilon_{eo}L_{bl}/L_{eo})$, where ε_{eo} and ε_{bl} are the ambient temperature

dielectric constant at 1 kHz, and L_{eo} and L_{bl} are the thicknesses of E-O polymer and barrier layer, respectively; [*e*] Φ is the order parameters of poled samples, which is described as $\Phi = 1 - A/A_0$, where A_0 and A are the integral absorbance for the unpoled and poled films at normal incidence; [*f*] E_{equiv} is the effective electric field strength of pyroelectric poling.

As summarized in **Table 4-I**, very efficient poling from pyroelectric field generation was achieved compared to those results obtained from conventional contact poling. Equivalent electric fields up to 90 $V/\mu m$ were achieved during pyroelectric poling. The efficiency of pyroelectric field harvesting is determined by the ratio of E_{equiv} and E_{theo}. Very high E_{equiv}/E_{theo} ratios (85% – 100%) and relatively large r_{33} values (up to 81 pm/V at the wavelength of 1.31 μm) were obtained with uniformly poled films. The highest field strength harvested from pyroelectric poling, 90 $V/\mu m$ from LT and 47 $V/\mu m$ from LN, were almost linearly proportional to the γ values of two crystals.This study demonstrated the first sample of utilizing pyroelectric effect to pole E-O polymers.

Due to the transient nature of pyroelectric charges, the insertion of both PDMS and a barrier layer (PVP or P(VDF-TrFE)) was necessary to prevent charges from leaking through the E-O polymer, which has a relatively low resistivity. This can be exemplified by comparing the poling efficiency between triple-layered (entries 1-5 and 7, **Table 4-I**) and double-layered samples (entries 6 and 8, **Table 4-I**). In addition to providing soft contact lamination, PDMS also functioned as an insulating dielectric with stable electrical properties over a wide range of temperatures,[26] which was one of the key factors in maintaining durability of pyroelectric charges on the Z^+ face of crystals during poling.

Equally important, the insertion of a barrier layer (PVP or P(VDF-TrFE)) between the E-O polymer and ITO on the other side was also needed in order to stabilize the pyroelectric charges from the Z^- face of crystals. Although the resistivity of PVP and P(VDF-TrFE)[27-28] are comparable to that of **AJLZ53/PMMA**, significant charge trapping was expected at the interfaces between the adjacent dielectric layers following the Maxwell-Wagner polarization process,[29] which prevented charges from leaking through the polar surfaces of pyroelectric crystals. It should be mentioned that the triple-layered structure of pyroelectric poling is generally applicable to the poling of conventional waveguide devices where E-O polymers are usually poled in the parallel-plate (transverse) configuration.[30]

4.4 Experimental studies on slot-waveguide based ring-resonator modulator

To investigate the feasibility of pyroelectric poling in real devices with complicated geometry, we selected the same device configuration in a silicon-polymer hybrid slot waveguide ring-resonator modulator as reported earlier (**Figure 4-7A**).[9] The hybrid slot waveguide devices are expected to be one of the key components that will enable high-speed optical modulation with low driven voltages and small footprints.[31-32] In this study, the geometry of the strip-loaded slot waveguide utilized for the modulator consists of 230 nm wide arms, and a 200 nm slot width. The ring resonators constructed out of this waveguide possess a bend radius of 60 μm.

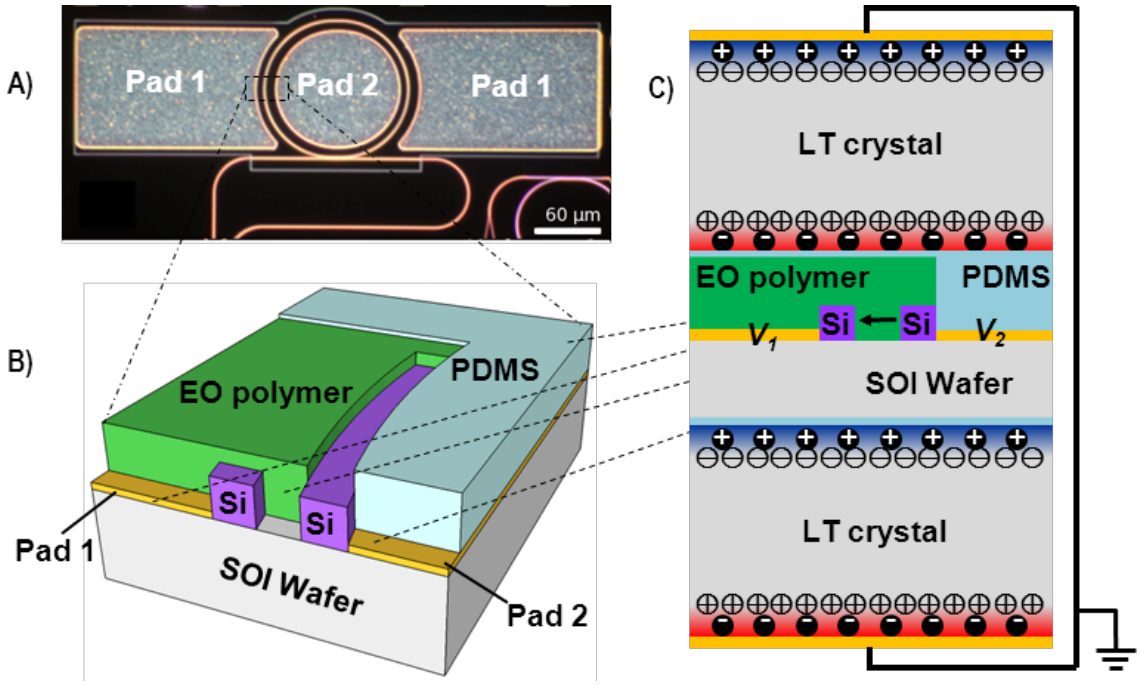

Figure 4-7. Pyroelectric poling of EO polymers in hybrid E-O polymer silicon slot waveguide ring-resonator modulators: A) dark field optical micrograph of the device; B) the partial cutaway view illustration of heterogeneous dielectric structures. A quasi-longitudinal polarization of the EO polymer is induced across the gap of two silicon slots, and the details of the hybrid structures are simplified to highlight the principal dielectric materials and electrical contact pads in the system for electrostatics analysis; C) the cross-sectional side view illustration of heterogeneous dielectric structures. The middle arrow in the silicon slot denotes the direction of electric fields within the slot during pyroelectric poling. Not to scale.

To compare with conventional poling, a reference device was poled at 100 V/µm across the slot by applying the poling voltage to the central pad (pad 2) and holding the outer two pads (pad 2) as ground. The DC tunability of the resonance wavelength device was determined to be 16.5 ± 0.6 pm/V by measuring transmission as a function of wavelength with the device biased at

several DC voltages. This level of tunability is substantial to quantify the r_{33} values of E-O films that were poled at the in-plane geometry. The implied in-slot r_{33} value of 19 pm/V at 1.55 μm as compared to the peak value of 60 pm/V from contact-poled thin films, indicating low poling efficiency of the polymer in slot waveguides.[9]

By design, the ring resonator needs to be poled in the in-plane configuration for E-O modulation. In order to create such in-plane polarization across the slot by using Z-cut LT crystal, a heterogeneous structure of dielectrics has been fabricated (**Figure 4-7 B** and **C**). The chip was initially coated with a micron-thick layer of **AJLZ53**/PMMA, and the material was cleared from the central pad 2 using a laser ablation system, leaving the bare area that was re-coated with PDMS. The thickness of PDMS was controlled to be slightly thicker than that of E-O polymer, which provides the soft-contact lamination with the Z^+ surface of a LT crystal. A secondary LT crystal is laminated at the bottom Z^- surface with an ultrathin spin-on PDMS layer. With the insertion of relatively thick (~1mm) SOI wafer, such a sandwiched structure between two crystals can generate higher effective field strength during pyroelectric poling than using a single crystal, while keeping the design of photonic dies unchanged. It also removes the potential complications of using the configured probe to ground one of the pads and adding an extra dielectric layer to the slot, which are very difficult to carry out in the 1cm x 2cm photonic die containing thousands of components.[33] The poling of the stack follows the same protocol that was used for poling thin film samples. The in-plane poling of E-O polymer across the slot is induced by the potential difference between two pads, due to the difference in dielectric constants between PDMS (2.86) and E-O polymer (~4.0).

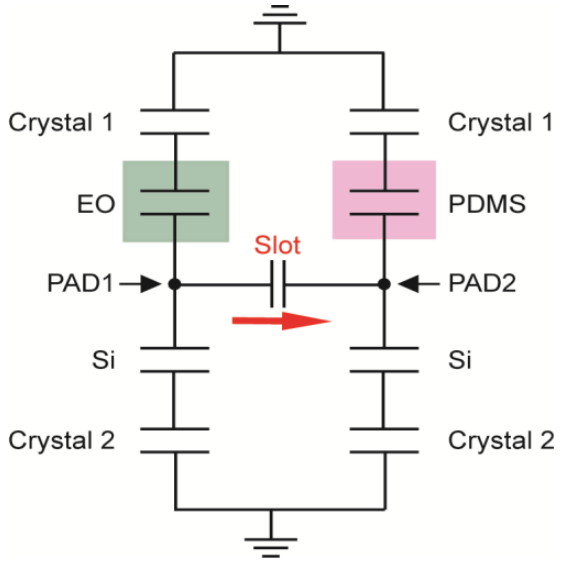

Figure 4-8. Simplified equivalent circuit of the ring resonator device.

To estimate the field strength of pyroelectric poling across the slot, we assume that the generated pyroelectric charges do not flow on the surfaces of LT crystals due to its high resistivity. A simplified equivalent circuit of this slot waveguide based ring resonator, as shown in **Figure 4-8**, was used to estimate the field strength during pyroelectric poling. The electric field in the design of heterogeneous dielectrics can be described by

$$E_{di} = 2\gamma\Delta T\varepsilon_0^{-1}[2\varepsilon_{di} + \varepsilon_{cr}L_{di}/L_{cr} + L_{si}\varepsilon_{cr}\varepsilon_{di}/(L_{cr}\varepsilon_{si})]^{-1} \quad \textbf{(4-2)}$$

$$E_{cr} = \gamma\Delta T(L_{sw}\varepsilon_{di} + L_{di}\varepsilon_{si})\,[\varepsilon_0\,(L_{sw}\varepsilon_{di}\,\varepsilon_{cr} + L_{di}\,\varepsilon_{cr}\,\varepsilon_{si} + 2L_{cr}\varepsilon_{si}\varepsilon_{di})]^{-1} \quad \textbf{(4-3)}$$

where the parameters (ε_{di} and L_{di}) of dielectric materials are those of PDMS and E-O polymer, ε_{si} is the dielectric permittivities of silicon, and L_{sw} is the thickness of the SOI wafer, respectively. The electric field from the grounded top surface to the pad is integrated to give the electric

potentials on pad 1 and pad 2, respectively, resulting in a potential difference of 29 V across the 200 nm slot and electric field strength of 145 V/μm through the pyroelectric poling.

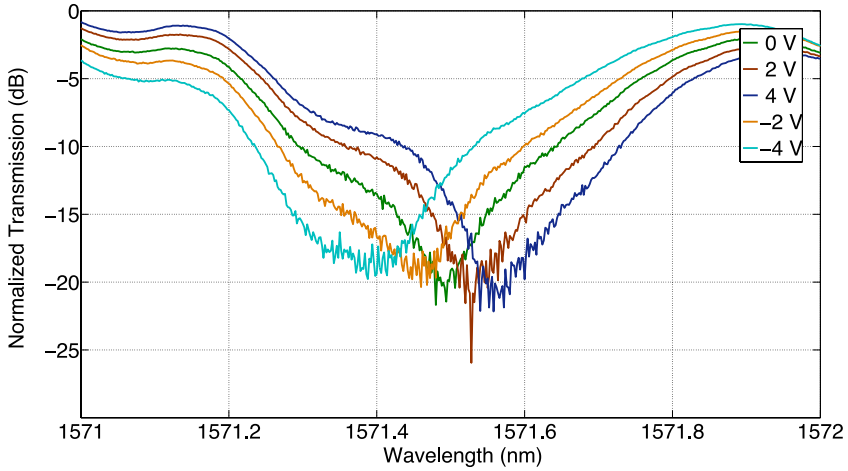

Figure 4-9. Spectrum at various bias voltages on pyroelectrically poled hybrid slotwaveguide ring-resonator. It shows a tunability of 25 pm/V.

The DC tunability of the device was determined by measuring transmission as a function of wavelength (around 1571 nm) using a low-speed optical power detector with the device biased at several DC voltages. This was done in a non-sequential fashion to exclude thermal drift as the cause of the peak shifting behavior. (**Figure 4-9**) After pyroelectric poling and separation of the die from the LT crystal, the device shows a DC resonance wavelength tunability of 25 pm/V. This result is 60% higher than those obtained from contact-poled devices and it exceeds the best value reported for depletion-based ring modulators.[34] High-frequency measurements were taken with a high frequency avalanche photodiode (APD). The optical wavelength of the ring is biased at the location of the steepest slope in the resonator wavelength spectrum and the drive signal was kept sufficiently small to ensure a linear response of the device. The ratio of the system

detected RF power to the input RF power is used to measure the RF performance of the device. The S_{21} parameter relating the output to the input is indicating a 6 dB roll-off at around 800 MHz. This point corresponds to the half-power in the electro-optic response of the device and is a standard measure of the RF bandwidth. This 6 dB electrical bandwidth at 800 MHz is a conclusive evidence of the E-O modulation for enhanced tunability of slot waveguides. The improved device performance and high electric field strength observed in this study indicate the great promises of using pyroelectric poling to introduce the in-plane polarization of E-O polymers that are essential to various designs of hybrid photonic devices.

4.5 Conclusion

In summary, we demonstrated a novel process using surface-modified LT and LN crystals as an effective conformal and detachable electric field source for efficient poling of E-O polymers. The employment of this approach not only helps to avoid the severe leakage current associated with conventional poling, but also provides poled devices with better uniformity and processibility. Through the modest temperature changes of pyroelectric crystals and careful design of heterogeneous dielectric systems, very large electric fields (50 - 350 V/μm) can be generated in both transverse and longitudinal configurations. More importantly, these high electric fields can be applied to amorphous dielectric films with a broad thickness variation. Considering that the polar surfaces of pyroelectric crystals are patternable and switchable [16], we expect that the electric field generated from pyroelectrics can be used to greatly facilitate the development of polarization-dependent functional materials and devices.

Notes to Chapter 4

[1] R. Blum, M. Sprave, J. Sablotny, M. Eich, *Journal of the Optical Society of America B* 1998, **15**, 318.

[2] S. Huang, T. D. Kim, J. D. Luo, S. K. Hau, Z. W. Shi, X. H. Zhou, H. L. Yip, A. K. Y. Jen, *Applied Physics Letters* 2010, **96**, 243311.

[3] D. M. Burland, R. D. Miller, C. A. Walsh, *Chemical Reviews* 1994, **94**, 31.

[4] M. A. Mortazavi, A. Knoesen, S. T. Kowel, B. G. Higgins, A. Dienes, *Journal of the Optical Society of America B* 1989, **6**, 733.

[5] M. Sprave, R. Blum, M. Eich, *Applied Physics Letters* 1996, **69**, 2962.

[6] R. A. Hill, A. Knoesen, M. A. Mortazavi, *Applied Physics Letters* 1994, **65**, 1733.

[7] T. Baehr-Jones, B. Penkov, J. Huang, P. Sullivan, J. Davies, J. Takayesu, J. Luo, T.-D. Kim, L. Dalton, A. Jen, M. Hochberg, A. Scherer, *Appled Physics Letters* 2008, **92**, 163303.

[8] R. Ding, T. Baehr-Jones, Y. Liu, R. Bojko, J. Witzens, S. Huang, J. Luo, S. Benight, P. Sullivan, J. M. Fedeli, M. Fournier, L. Dalton, A. Jen, M. Hochberg, *Optics Express* 2010, **18**, 15618.

[9] M. Gould, T. Baehr-Jones, R. Ding, S. Huang, J. Luo, A. K. Y. Jen, J.-M. Fedeli, M. Fournier, M. Hochberg, *Optics Express* 2011, **19**, 3952.

[10] G. Rosenman, D. Shur, Y. E. Krasik, A. Dunaevsky, *Journal of Applied Physics* 2000, **88**, 6109.

[11] Y. Watanabe, M. Okano, A. Masuda, *Physical Review Letters* 2001, **86**, 332.

[12] Y. Yun, E. I. Altman, *Journal of the American Chemical Society* 2007, **129**, 15684.

[13] D. B. Li, M. H. Zhao, J. Garra, A. M. Kolpak, A. M. Rappe, D. A. Bonnell, J. M. Vohs, *Nature Materials* 2008, **7**, 473.

[14] K. Garrity, A. M. Kolpak, S. Ismail-Beigi, E. I. Altman, *Advanced Materials* 2010, **22**, 2969.

[15] D. Ehre, E. Lavert, M. Lahav, I. Lubomirsky, *Science* 2010, **327**, 672.

[16] P. Ferraro, S. Grilli, L. Miccio, V. Vespini, *Applied Physics Letters* 2008, **92**, 213107.

[17] J. D. Brownridge, S. M. Shafroth, *Applied Physics Letters* 2001, 79, 3364.

[18] J. Geuther, Y. Danon, F. Saglime, *Physical Review Letters*, 2006, **96**, 054803.

[19] B. Naranjo, J. K. Gimzewski, S. Putterman, *Nature* 2005, **434**, 1115.

[20] T. Z. Fullem, Y. Danon, *Joural of Applied Physics* 2009, **106**, 074101.

[21] T. Z. Fullem, K. C. Fazel, J. A. Geuther, Y. Danon, *Radiation Research* 2009, **172**, 643.

[22] S. B. Lang, *Physics Today* 2005, **58**, 31.

[23] C. C. Teng, H. T. Man, *Applied Physics Letters* 1990, **56**, 1734.

[24] D. H. Park, C. H. Lee, W. N. Herman, *Optics Express* 2006, **14**, 8866.

[26] R. Bartnikas, Electrical Insulation, IEEE Transactions on 1967, **EI-2**, 33.

[27] S. L. Seokhwan Bang, Sunyeol Jeon, Semyung Kwon, Wooho Jeong, Honggyu Kim, Iksup Shin, Ho Jung Chang, Hyung-ho Park and Hyeongtag Jeon, *Semiconductor Science and Technol*ogy 2009, **24**, 025008.

[28] K. Müller, I. Paloumpa, K. Henkel, D. Schmeisser, *Journal of Applied Physics*, 2005, **98**, 056104.

[29] G. C. Montanari, P. H. F. Morshuis, *Dielectrics and Electrical Insulation*, IEEE Transactions on 2005, **12**, 754.

[30] Y. Enami, C. T. Derose, D. Mathine, C. Loychik, C. Greenlee, R. A. Norwood, T. D. Kim, J. Luo, Y. Tian, A. K. Y. Jen, N. Peyghambarian, *Nature Photonics* 2007, **1**, 180.

[31] T. Baehr-Jones, M. Hochberg, *Nature Photonics* 2009, **3**, 193.

[32] J. Leuthold, C. Koos, W. Freude, *Nature Photonics* 2010, **4**, 535.

[33] M. Hochberg, T. Baehr-Jones, *Nature Photonics* 2010, **4**, 492.

[34] P. Dong, S. Liao, D. Feng, H. Liang, D. Zheng, R. Shafiiha, C.-C. Kung, W. Qian, G. Li, X. Zheng, A. V. Krishnamoorthy, M. Asghari, *Optics Express* 2009, **17**, 22484.

Chapter 5. Pyroelectric poling of electro-optic polymer thin films through a thick insulating substrate

5.1 Background and motivation

In Chapter 4 we have discussed the feasibility of using pyroelectric poling to introduce chromophore alignment to organic EO materials in both micron-thick thin film and hybrid slot waveguide modulator devices. In thin films, we have seen results comparable to those from contact-poled samples. However, in slot waveguide devices, pyro-poled samples showed a 60% improvement over those contact-poled devices. These results underline the great processibility and potential application flexibility of the pyroelectric poling method. We suggest that this advantage in processibility and flexibility can benefit to a much broader variety of applications, which were originally very difficult to handle with conventional contact poling or corona poling.

As has been mentioned previously, in order to break the centrosymmetry that naturally exists in these amorphous polymeric materials, an electric field of 10^{7-8} V/m is needed to efficiently orient the dipolar chromophores at elevated temperature.[1-2] In polymer based photonic devices, E-O polymer is usually sandwiched between two dielectric claddings, which confine the optical mode within the core layer and separate the mode from the conductive electrodes.[3-4] It has been a long-existing challenge for researchers to effectively deliver the necessary electric field to the active core layer during the poling of these multilayer structures.[5] In the past, this electric field was most commonly applied using an external high voltage power supply through contacting

electrodes. The poling voltage distributes in this 3-layer structure according to the resistors-in-series model, which means the claddings can dissipate a considerable amount of voltage if it is not much more conductive than the core layer.[6] However, more conductive cladding also brings the risk of increasing dielectric loss and optical loss.[7] Thus a careful engineering choice must be made to balance these two aspects, along with many other requirements such as suitable dielectric constant, refractive index and process adaptability.[8] Confined by all these stringent restraints, the possible material choice for multilayer photonic devices is very limited. The situation can be partially improved if the waveguide structure can be first poled with only the bottom cladding before the application of the top cladding. In this case only the properties of the bottom cladding remain a concern. However, it would be more plausible if there is a method to efficiently pole E-O polymer core regardless the resistance of the cladding, because such a method can largely expand the freedom of device design.

Recently we reported an alternative poling method, which utilizes pyroelectric crystals instead of external power supply and conductive electrodes to effectively pole E-O polymers.[9] This pyro- poling may have opened up new possibilities to pole multilayer polymer waveguide structures. The principal of this method is that pyroelectric crystals can develop strong surface depolarization field upon temperature perturbation.[10-11] Under a thermal treatment carefully designed to match the poling temperature requirements, this depolarization field can be as high as 3.5×10^8 V/m in polymer thin films in close contact with a standard z-cut lithium tantalate (LT) crystal, which is more than adequate for the poling of E-O polymers.[9] One major advantage of this depolarization field is that it is generated from the disrupted equilibrium between the spontaneous polarization (P_s) and the surface screening charge (σ_s), both of which are much less mobile than the carriers injected from the conductive electrodes.[10-12] Thus the voltage

distribution under this method literally follows the capacitors-in-series model because of the long circuit RC relaxation time,[7] which makes the use of very insulating cladding layers a possible choice. In this dissertation, we demonstrated an extreme scenario, in which E-O polymer films were poled with 3 orders thicker dielectric layer in circuit, producing electro-optic coefficients (r_{33}s) up to 62 pm/V. To reach equivalent results in the same structure using contact poling, an electric field of 53 kV is needed. Theoretical analysis indicates that these results are very close to the ideal zero leakage current poling and can be significantly improved if the substrate has higher dielectric constant or is thinner.

5.2 Experimental studies and discussion

The E-O polymer used in this study was a guest-host system formulated by doping 15 wt% of a dipolar phenyltetraene chromophore AJLZ53 into PMMA. The polymer composite had a DSC measured T_g at 110 °C.[9] When poled in single layer thin film with 10^8V/μm electric field using contact poling, this material exhibited a maximum r_{33} of ~90 pm/V at 1.31 μm. 1mm thick z-cut lithium niobate (LN, γ_{LN}=83 μC/(m^2·°C)) and lithium tantalate (γ_{LT}=176 μC/(m^2·°C))crystals were used for the poling.[11] As has been elaborated in the previous study, the air-gap-free contact between the detachable crystals and the polymer sample is one critical requirement for the success of pyro-poling.[9] Thus on each contacting surface, a 70 nm thick polydimethylsiloxane (PDMS) elastomer layer was applied before we assembled the poling stacks. The poling procedure is described in **Figure 5-1**. First of all, the E-O polymer film (1-2 μm) was prepared on an ITO (40 nm)/glass (1mm) substrate by spin-coating. After overnight baking in vacuum oven, gold electrode was sputtered on this thin film. It is worth noting that both the ITO and gold electrodes were not used in the pyro-poling process and were just optional. They were included in the test device merely to facilitate the simple Teng-Man r_{33} measurement after pyro-poling.[13-

[14] The E-O polymer film together with the glass substrate was then sandwiched between two z-cut pyroelectric crystals. The crystal on top contacted the E-O polymer with its z^+ surface under the help of the PDMS layer and the bottom crystal stuck to the back side of the glass substrate with its z^- surface. The orientations of the two crystals were thus consistent. Then both the top and the bottom surfaces of the whole stack were connected and grounded to close the circuit. After that, this poling stack was put into a hot plate and exposed to the designed thermal treatment. We found that it worked the best if we heated the sample up first to a maximum temperature (T_m) above T_g, held it until the σ_s and P_s reached a new equilibrium and then cooled it down rapidly. After the sample reached the room temperature, the crystals were carefully peeled off and the residue PDMS on E-O polymer was carefully cleaned with Q-tip and isopropyl alcohol. The crystals can be re-used after cleaning.

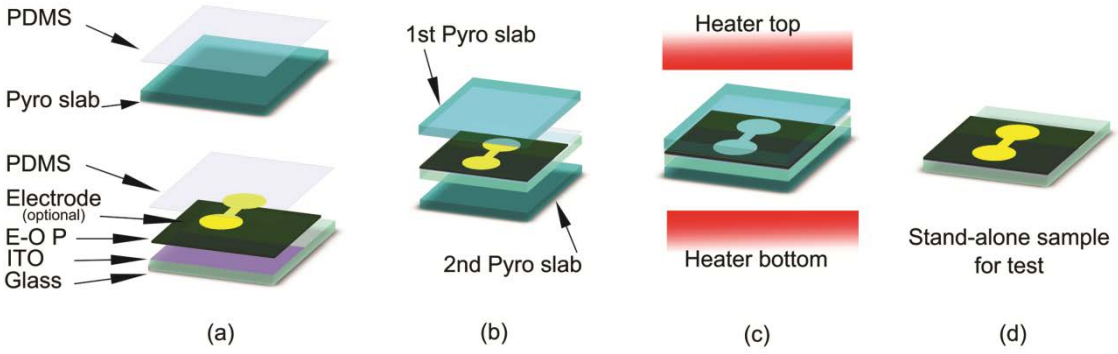

Figure 5-1. Procedures to pole E-O polymer thin films with thick glass substrate in circuit using pyro-poling. **a**, layers of E-O polymer, electrode (optional), and PDMS were sequentially processed onto ITO substrate while the same PDMS layer was coated on the crystals. **b**, the substrate with E-O polymer was sandwiched between two pyroelectric crystals. **c**, the whole stack was exposed to a pre-programmed thermal treatment. **d**, after the sample was cooled down to room temperature, crystals and PDMS were removed, leaving the stand-alone sample ready for test.

A series of pyro-poling tests were performed with different T_m using both LT crystals and LN crystals. The r_{33}s were measured at 1.31 μm using simple Teng-Man reflection technique.[13-14] Notable E-O activities were observed on these pyro-poled films. In **Figure 5-2**, the r_{33}s are first plotted versus T_m and then compared to contact-poled single layer E-O polymer film to extract the effective field obtained inside the E-O layer during the pyro-poling.

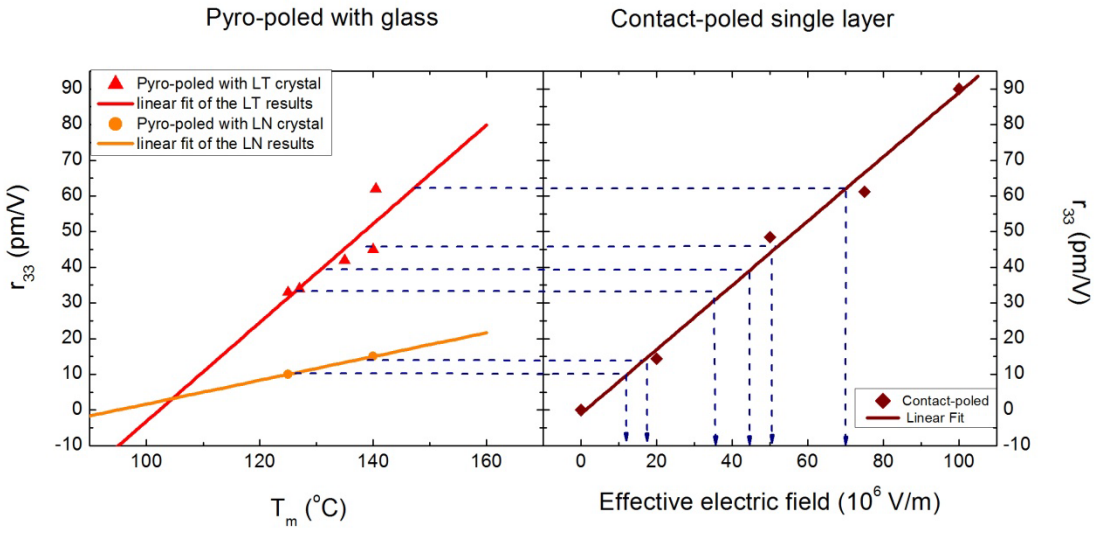

Figure 5-2. Left, r_{33}s of E-O polymer thin films poled by pyroelectric crystals at different maximum temperatures. The scattered symbols were from experiments and the lines were from linear fitting. Right, same polymer poled in single layer structure using contact poling at different poling electric fields ranging from 0.2-1.0×10^8 V/m. Data from the left were used to extract the effective poling field generated during pyro-poling.

It can be seen from **Figure 5-2** that the pyro-poled films showed r_{33}s ranging from 10 pm/V to 62 pm/V. The r_{33}s increased almost linearly with $\Delta T=(T_m-T_0)$, where T_0 was 99 °C. The highest

T_m we tried was 145 °C, because higher temperature can bring more complicated morphological and compositional changes to the film. The $r_{33}/(T_m-T_0)$ slopes for the two different crystals used were 0.33 for LN and 1.38 for LT respectively. These numbers partially reflected the different pyroelectric coefficients of the two crystals, which are γ_{LN} =83 μC/(m^2·°C) and γ_{LT}=176 μC/(m^2·°C). The effective electric field obtained during the pyroelectric poling were 1.2-1.8×10^7 V/m for LN crystals and 3.6-7.0×10^7 V/m for LT crystals. If we consider the resistivity of the E-O layer and the glass substrate are 1.3×10^9 Ω·m and 10$^{10\text{-}14}$ Ω·m respectively, as well as the thickness contrast 1 μm:1 mm, this is almost impossible to pole if contact poling is used following resistors-in-series model. On the other hand, even if capacitors-in-series model is used, it would need a total of 53 kV to pole with contact poling, considering the low frequency dielectric constants of the E-O layer and the glass are 3.5 and 4.6 respectively. The most interesting aspect is that this poling were done from outside of the thick insulating substrate, with the testing electrodes left floating during the whole poling process.

It is interesting how these small pyroelectric crystals can generate such high equivalent electric field. In our previous studies, we have theoretically demonstrated how surface depolarization field up to 3.5 ×10^8 V/m is generated by LT crystals through moderate temperature change, where **Equation (1)** applies.[15]

$$E_{di} = \frac{\gamma(T)\Delta T}{\varepsilon_0} \times \frac{1}{\left(\varepsilon_{di} + \frac{d_{di}}{d_{cr}}\varepsilon_{cr}\right)} \qquad (\mathbf{5\text{-}1})$$

The subscripts *di* and *cr* stand for the dielectric material (E-O polymer) and the crystal respectively. However, **Equation (1)** is valid only when the E-O polymer is directly on top of a pyroelectric crystal and no other dielectric layer is in the circuit. We have shown that with a very

thin barrier layer inserted between E-O polymer and the crystal, ~90% theoretical field can be harvested during pyro-poling.[9] However, the results reported in this letter cannot be directly interpreted by **Equation (5-1)** because of the presence of the thick glass layer. The structure and equivalent circuit of the poling device are summarized in Figure 3 (a) and (b). If the poling stack is subjected to a temperature change ΔT, on every unit area charges will distribute within the stack as shown in Figure 3 (b). Thus under equilibrium condition, the ideal electric field generated in the E-O layer can be calculated using **Equation (5-2).**

$$E_{EO} = \frac{2\gamma(T)\Delta T}{\varepsilon_0\left(2\varepsilon_{EO} + \frac{d_{EO}}{d_{cr}}\varepsilon_{cr} + \frac{d_{glass}\varepsilon_{cr}\varepsilon_{EO}}{d_{cr}\varepsilon_{glass}}\right)} \qquad \textbf{(5-2)}$$

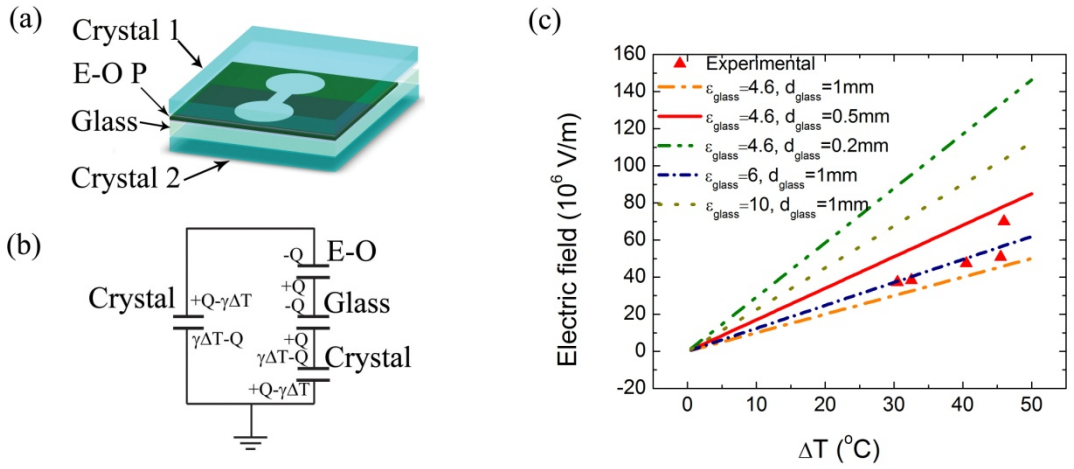

Figure 5-3. (a) Structure and (b) equivalent circuit of the pyro-poling device. (c) Theoretical electric field calculated using **Equation (5-2)** on different insulating substrates. ε_{EO}=3.5, ε_{cr}=43 and γ=176 μC/(m^2·°C) for LT crystal were used in calculation.

In **Figure 5-3 (c)**, we calculated the theoretical electric field generated in E-O layer during pyro-poling on insulating substrates with different thickness and dielectric constants. The crystal used in the calculation was LT. The polymer thickness was fixed at 1 μm. It can be seen that the experiment results are very close to the calculation, which suggests that our pyro-poling was efficient and close to the ideal no leaking situation. On the other hand, one can see that higher electric field can be obtained under the same temperature change ΔT if the substrate has higher dielectric constant or the thickness is reduced. For a 0.2 mm thick glass substrate with ε_{glass}=4.6, 35 °C temperature change can give 10^8V/m effective poling field within the EO layer. For a 1 mm dielectric substrate with ε=10, the same effective poling field can be reached with ΔT=45°C. These results suggest that pyroelectric poling in this geometry can be readily improved by slightly adjust the substrate parameters, not to mention there exist pyroelectric crystals better than LT.[11]

5.3 Conclusion

In summary, we have demonstrated a method to efficiently pole E-O polymers using pyroelectric crystals from outside of a thick insulating substrate, with the testing electrodes left floating during the whole poling process. The electric potential generated from such pyroelectric crystals during poling can reach several tens of kilovolts, which is enough to induce 7×10^7 V/m electric field in the 1 μm E-O layer and produce r_{33}s up to 62 pm/V. The experiment results match well with the theoretical estimation, which also suggests that the poling electric field can be improved by using substrates with higher dielectric constant or lower thickness. 10^8 V/m poling field can be expected with minor changes. These findings provide an alternative way to

efficiently pole E-O polymers in novel photonic devices with multilayer structure containing dielectric substrates. This demonstration may also open up new processing strategies for functional dielectrics and their hybrid systems to be used in a broad spectrum of electronic and photonic applications.

Notes to Chapter 5

[1] L. R. Dalton, W. H. Steier, B. H. Robinson, C. Zhang, A. Ren, S. Garner, A. Chen, T. Londergan, L. Irwin, B. Carlson, L. Fifield, G. Phelan, C. Kincaid, J. Amend and A. Jen, *Journal of Materials Chemistry* 1999, **9**, 1905.

[2] D. M. Burland, R. D. Miller and C. A. Walsh, *Chemical Reviews* 1994, **94**, 31.

[3] C. T. DeRose, Y. Enami, C. Loychik, R. A. Norwood, D. Mathine, M. Fallahi, N. Peyghambarian, J. D. Luo, A. K.-Y. Jen, M. Kathaperumal and M. Yamamoto, *Applied Physics Letters* 2006, **89**, 131102.

[4] H. Ma, A. K. Y. Jen and L. R. Dalton, *Advanced Materials* 2002, **14**, 1339.

[5] J. Luo, S. Huang, Z. Shi, B. M. Polishak, X.-H. Zhou and A. K. Y. Jen, *Chemistry of Materials* 2010, **23**, 544.

[6] J. G. Grote, J. S. Zetts, R. L. Nelson, F. K. Hopkins, L. R. Dalton, C. Zhang and W. H. Steier, *Optical Engineering* 2001, **40**, 2464.

[7] L. Bing, R. Dinu, J. Dan, H. Diyun, C. Baoquan, A. Barklund, E. Miller, M. Moolayil, Y. Guomin, F. Yun, Z. Lixin, C. Hui and J. Vemagin, presented at the *Optical Fiber Communication and Optoelectronics Conference*, Asia, 2007 .

[8] Y. Enami, C. T. Derose, D. Mathine, C. Loychik, C. Greenlee, R. A. Norwood, T. D. Kim, J. Luo, Y. Tian, A. K. Y. Jen and N. Peyghambarian, *Nature Photonics* 2007, **1**, 180.

[9] S. Huang, J. Luo, H.-L. Yip, A. Ayazi, X.-H. Zhou, M. Gould, A. Chen, T. Baehr-Jones, M. Hochberg and A. K. Y. Jen, *Advanced Materials* 2012, **24**, OP42.

[10] G. Rosenman, D. Shur, Y. E. Krasik and A. Dunaevsky, *Journal of Applied Physics* 2000, **88**, 6109.

[11] S. B. Lang, *Physics Today* 2005, **58**, 31.

[12] Y. Watanabe, M. Okano and A. Masuda, *Physical Review Letters* 2001, **86**, 332.

[13] C. C. Teng and H. T. Man, Applied Physics Letters 1990, **56**, 1734.

[14] D. H. Park, C. H. Lee and W. N. Herman, Optical Express 2006, **14**, 8866.

[15] D. Gillich, A. Kovanen, B. Herman, T. Fullem and Y. Danon, Nuclear Instruments and Methods A 2009, **602**, 306.

Bibliography

1. D. M. Burland, R. D. Miller, C. A. Walsh, *Chemical Reviews* 1994, **94**, 31.
2. L. R. Dalton, W. H. Steier, B. H. Robinson, C. Zhang, A. Ren, S. Garner, A. Chen, T. Londergan, L. Irwin, B. Carlson, L. Fifield, G. Phelan, C. Kincaid, J. Amend, A. Jen, *Journal of Materials Chemistry* 1999, **9**, 1905.
3. M. Hochberg, T. Baehr-Jones, G. Wang, M. Shearn, K. Harvard, J. Luo, B. Chen, Z. Shi, R. Lawson, P. Sullivan, A. K. Y. Jen, L. Dalton, A. Scherer, *Nature Materials* 2006, **5**, 703.
4. C. V. McLaughlin, L. M. Hayden, B. Polishak, S. Huang, J. D. Luo, T. D. Kim, A. K. Y. Jen, *Applied Physics Letters* 2008, **92**, 151107.
5. L. R. Dalton, *Journal of Physics: Condensed Matter* 2003, **15**, R897.
6. L. Dalton, *Polymers for Photonics Applications I, Advances in Polymer Science*, **Vol. 158** (Ed: K.-S. Lee), Springer Berlin / Heidelberg, 2002, 1.
7. M. J. a. P. Gunter, *Introduction to Organic Electronic and Optoelectronic Materials and Devices*, CRC Press, Boca Raton, Florida 2008.
8. J. Oudar, *Journal of Chemical Physics* 1977, **66**, 2664.
9. S. R. Marder, L.-T. Cheng, B. G. Tiemann, A. C. Friedli, M. Blanchard-Desce, J. W. Perry, J. Skindhøj, *Science* 1994, **263**, 511.
10. G. Bourhill, J.-L. Bredas, L.-T. Cheng, S. R. Marder, F. Meyers, J. W. Perry, B. G. Tiemann, *Journal of the American Chemical Society* 1994, **116**, 2619.
11. Y. Shi, C. Zhang, H. Zhang, J. H. Bechtel, L. R. Dalton, B. H. Robinson, W. H. Steier, *Science* 2000, **288**, 119.
12. L. Dalton, S. Benight, *Polymers* 2011, **3**, 1325.

13. C. T. DeRose, Y. Enami, C. Loychik, R. A. Norwood, D. Mathine, M. Fallahi, N. Peyghambarian, J. D. Luo, A. K.-Y. Jen, M. Kathaperumal, M. Yamamoto, *Applied Physics Letters* 2006, **89**, 131102.
14. C. T. Derose, R. Himmelhuber, D. Mathine, R. A. Norwood, J. Luo, A. K. Y. Jen, N. Peyghambarian, *Optics Express* 2009, **17**, 3316.
15. Y. Enami, C. T. Derose, D. Mathine, C. Loychik, C. Greenlee, R. A. Norwood, T. D. Kim, J. Luo, Y. Tian, A. K. Y. Jen, N. Peyghambarian, *Nature Photonics* 2007, **1**, 180.
16. M. Gould, T. Baehr-Jones, R. Ding, S. Huang, J. Luo, A. K. Y. Jen, J.-M. Fedeli, M. Fournier, M. Hochberg, *Optics Express* 2011, **19**, 3952.
17. B. A. Block, T. R. Younkin, P. S. Davids, M. R. Reshotko, P. Chang, B. M. Polishak, S. Huang, J. D. Luo, A. K. Y. Jen, *Optics Express* 2008, **16**, 18326.
18. B. Bartosz, H. Yu-Chueh, T. Hidehisa, S. Byoung-Joon, L. Jingdong, K. Y. J. Alex, H. S. William, R. F. Harold, *Selected Topics in Quantum Electronics*, IEEE Journal of 2007, **13**, 104.
19. M. Ieda, *IEEE Transactions on Electrical Insulation* 1980, **EI-15**, 206.
20. S. Huang, T. D. Kim, J. D. Luo, S. K. Hau, Z. W. Shi, X. H. Zhou, H. L. Yip, A. K. Y. Jen, *Applied Physics Letters* 2010, **96,** 243311.
21. J. Luo, S. Huang, Z. Shi, B. M. Polishak, X.-H. Zhou, A. K. Y. Jen, *Chemistry of Materials* 2010, **23**, 544.
22. M. Sprave, R. Blum, M. Eich, *Applied Physics Letters*, 1996, **69**, 2962.
23. R. Blum, M. Sprave, J. Sablotny, M. Eich, *Journal of the Optical Society of America B* 1998, **15**, 318.

24. J. P. Drummond, S. J. Clarson, J. S. Zetts, F. K. Hopkins, S. J. Caracci, *Applied Physics Letters* 1999, **74**, 368.

25. J. G. Grote, J. S. Zetts, R. L. Nelson, F. K. Hopkins, L. R. Dalton, C. Zhang, W. H. Steier, *Optical Engineering* 2001, **40**, 2464.

26. D. H. Park, C. H. Lee, W. N. Herman, *Optics Express* 2006, **14**, 8866.

27. S. K. Hau, H.-L. Yip, O. Acton, N. S. Baek, H. Ma, A. K. Y. Jen, *Journal of Materials Chemistry* 2008, **18**, 5113.

28. T.-D. Kim, J. Luo, Y.-J. Cheng, Z. Shi, S. Hau, S.-H. Jang, X.-H. Zhou, Y. Tian, B. Polishak, S. Huang, H. Ma, L. R. Dalton, A. K. Y. Jen, *The Journal of Physical Chemistry C* 2008, **112**, 8091.

29. K. Hassan, et al., *Journal of Physics D: Applied Physics* 2003, **36**, 1120.

30. C. Teng, H. T. Man, *Applied Physics Letters* 1990, **56**, 1734.

31. M. Gratzel, *Nature* 2001, **414**, 338.

32. V. I. Arkhipov, H. V. Seggern, E. V. Emelianova, *Applied Physics Letters* 2003, **83**, 5074.

33. P. M. Borsenberger, L. Pautmeier, H. Bassler, *The Journal of Chemical Physics* 1991, **94**, 5447.

34. R. Agrawal, P. Kumar, S. Ghosh, A. K. Mahapatro, *Applied Physics Letters* 2008, **93**, 073311.

35. D. H. Dunlap, P. E. Parris, V. M. Kenkre, *Physical Review Letters* 1996, **77**, 542.

36. K. C. Kao, *Dielectric Phenomena in Solids*, Elsevier Academic Press, San Diego 2004.

37. C. C. Teng, M. A. Mortazavi, G. K. Boudoughian, *Applied Physics Letters* 1995, **66**, 667.

38. P. W. M. Blom, M. J. M. de Jong, M. G. van Munster, *Physical Review B* 1997, **55**, R656.

39. F. Michelotti, *Journal of Applied Physics* 1998, **83**, 7886.

40. M. Haller, J. Luo, H. Li, T.-D. Kim, Y. Liao, B. H. Robinson, L. R. Dalton, A. K. Y. Jen, *Macromolecules* 2004, **37**, 688.

41. Z. W. Shi, J. D. Luo, S. Huang, X. H. Zhou, T. D. Kim, Y. J. Cheng, B. M. Polishak, T. R. Younkin, B. A. Block, A. K. Y. Jen, *Chemistry of Materials* 2008, **20**, 6372.

42. Z. W. Shi, J. D. Luo, S. Huang, Y. J. Cheng, T. D. Kim, B. M. Polishak, X. H. Zhou, Y. Q. Tian, S. H. Jang, D. B. Knorr, R. M. Overney, T. R. Younkin, A. K. Y. Jen, *Macromolecules* 2009, **42**, 2438.

43. Z. W. Shi, W. Liang, J. D. Luo, S. Huang, B. M. Polishak, X. S. Li, T. R. Younkin, B. A. Block, A. K. Y. Jen, *Chemistry of Materials* 2010, **22**, 5601.

44. T.-D. Kim, J.-W. Kang, J. Luo, S.-H. Jang, J.-W. Ka, N. Tucker, J. B. Benedict, L. R. Dalton, T. Gray, R. M. Overney, D. H. Park, W. N. Herman, A. K. Y. Jen, *Journal of the American Chemical Society* 2007, **129**, 488.

45. B. M. Polishak, S. Huang, J. D. Luo, Z. W. Shi, X. H. Zhou, A. Hsu, A. K. Y. Jen, *Macromolecules* 2011, **44**, 1261.

46. W. Köhler, D. R. Robello, P. T. Dao, C. S. Willand and D. J. Williams, *Journal of Chemical Physics*, 1990, **93**, 9157.

47. G. Sessler, *Topics in Applied Physics* 1987, **33**, 13.

48. Navrotsky, *Geochemical Transactions* 2003, **4**, 34.

49. H. Zhang, J. F. Banfield, *Journal of Materials Chemistry* 1998, **8**, 2073.

50. V. Bune, V. M. Fridkin, S. Ducharme, L. M. Blinov, S. P. Palto, A. V. Sorokin, S. G. Yudin, A. Zlatkin, *Nature* 1998, **391**, 874.

51. T. B. Singh, F. Meghdadi, S. Günes, N. Marjanovic, G. Horowitz, P. Lang, S. Bauer, N. S. Sariciftci, *Advanced Materials* 2005, **17**, 2315.

52. X. Peng, G. Horowitz, D. Fichou, and F. Garnier, *Applied Physics Letters* 1990, **57**, 2013.

53. S. Wi, N. Senthilkumar, S. W. Rhee, *Journal of Materials Science-Materials in Electronics* 2008, **19**, 45.

54. V. Bharti, Q. M. Zhang, *Physical Review B* 2001, **63**, 184103.

55. Z. M. Dang, Y. H. Lin, C. W. Nan, *Advanced Materials* 2003, **15**, 1625.

56. P. Munzert, U. Schulz, N. Kaiser, *Surface and Coating Technology*, 2003, **174-175**, 1048.

57. R. D. Shannon, R. A. Oswald, G. R. Rossman, *Physics and Chemistry of Minerals* 1992, 19, 166.

58. J. S. Kim, J. H. Park, J. H. Lee, J. Jo, D. Y. Kim, and K. Cho, *Applied Physics Letters* 2007, **91**, 112111.

59. M. A. Mortazavi, A. Knoesen, S. T. Kowel, B. G. Higgins, A. Dienes, *Journal of the Optical Society of America B* 1989, **6**, 733.

60. R. A. Hill, A. Knoesen, M. A. Mortazavi, *Applied Physics Letters* 1994, **65**, 1733.

61. T. Baehr-Jones, B. Penkov, J. Huang, P. Sullivan, J. Davies, J. Takayesu, J. Luo, T.-D. Kim, L. Dalton, A. Jen, M. Hochberg, A. Scherer, *Appled Physics Letters* 2008, **92**, 163303.

62. R. Ding, T. Baehr-Jones, Y. Liu, R. Bojko, J. Witzens, S. Huang, J. Luo, S. Benight, P. Sullivan, J. M. Fedeli, M. Fournier, L. Dalton, A. Jen, M. Hochberg, *Optics Express* 2010, **18**, 15618.

63. G. Rosenman, D. Shur, Y. E. Krasik, A. Dunaevsky, *Journal of Applied Physics* 2000, **88**, 6109.

64. Y. Watanabe, M. Okano, A. Masuda, *Physical Review Letters* 2001, **86**, 332.

65. Y. Yun, E. I. Altman, *Journal of the American Chemical Society* 2007, **129**, 15684.

66. D. B. Li, M. H. Zhao, J. Garra, A. M. Kolpak, A. M. Rappe, D. A. Bonnell, J. M. Vohs, *Nature Materials* 2008, **7**, 473.

67. K. Garrity, A. M. Kolpak, S. Ismail-Beigi, E. I. Altman, *Advanced Materials* 2010, **22**, 2969.

68. D. Ehre, E. Lavert, M. Lahav, I. Lubomirsky, *Science* 2010, **327**, 672.

69. P. Ferraro, S. Grilli, L. Miccio, V. Vespini, *Applied Physics Letters* 2008, **92**, 213107.

70. J. D. Brownridge, S. M. Shafroth, *Applied Physics Letters* 2001, 79, 3364.

71. J. Geuther, Y. Danon, F. Saglime, *Physical Review Letters*, 2006, **96**, 054803.

72. B. Naranjo, J. K. Gimzewski, S. Putterman, *Nature* 2005, **434**, 1115.

73. T. Z. Fullem, Y. Danon, *Joural of Applied Physics* 2009, **106**, 074101.

74. T. Z. Fullem, K. C. Fazel, J. A. Geuther, Y. Danon, *Radiation Research* 2009, **172**, 643.

75. S. B. Lang, *Physics Today* 2005, **58**, 31.

76. R. Bartnikas, Electrical Insulation, IEEE Transactions on 1967, **EI-2**, 33.

77. S. L. Seokhwan Bang, Sunyeol Jeon, Semyung Kwon, Wooho Jeong, Honggyu Kim, Iksup Shin, Ho Jung Chang, Hyung-ho Park and Hyeongtag Jeon, *Semiconductor Science and Technol*ogy 2009, **24**, 025008.

78. K. Müller, I. Paloumpa, K. Henkel, D. Schmeisser, *Journal of Applied Physics*, 2005, **98**, 056104.

79. G. C. Montanari, P. H. F. Morshuis, *Dielectrics and Electrical Insulation*, IEEE Transactions on 2005, **12**, 754.

80. T. Baehr-Jones, M. Hochberg, *Nature Photonics* 2009, **3**, 193.

81. J. Leuthold, C. Koos, W. Freude, *Nature Photonics* 2010, **4**, 535.

82. M. Hochberg, T. Baehr-Jones, *Nature Photonics* 2010, **4**, 492.

83. P. Dong, S. Liao, D. Feng, H. Liang, D. Zheng, R. Shafiiha, C.-C. Kung, W. Qian, G. Li, X. Zheng, A. V. Krishnamoorthy, M. Asghari, *Optics Express* 2009, **17**, 22484.

84. H. Ma, A. K. Y. Jen and L. R. Dalton, *Advanced Materials* 2002, **14**, 1339.

85. L. Bing, R. Dinu, J. Dan, H. Diyun, C. Baoquan, A. Barklund, E. Miller, M. Moolayil, Y. Guomin, F. Yun, Z. Lixin, C. Hui and J. Vemagin, presented at the *Optical Fiber Communication and Optoelectronics Conference*, Asia, 2007 .

86. S. Huang, J. Luo, H.-L. Yip, A. Ayazi, X.-H. Zhou, M. Gould, A. Chen, T. Baehr-Jones, M. Hochberg and A. K. Y. Jen, *Advanced Materials* 2012, **24**, OP42.

87. D. Gillich, A. Kovanen, B. Herman, T. Fullem and Y. Danon, Nuclear Instruments and Methods A 2009, **602**, 306.

Curriculum Vitae

Su HUANG

Department of Materials Science & Engineering
University of Washington
302 Roberts Hall, Box 352120
Seattle, WA 98195-2120
(574) 302-5499
e-mail: huangsu@uw.edu

EDUCATION

Ph.D., Materials Science and Engineering: July 2012
University of Washington, Seattle, WA
Dissertation title: *Advanced processing methods to introduce and preserve dipole orientation in organic electro-optic materials for next generation photonic devices*
Advisor: Dr. Alex K.-Y. Jen

M.E., Materials Science and Engineering: June 2005
Nanjing University, Jiangsu, China
Dissertation title: *Preparation and characterization of ferroelectric inverse opal photonic crystals*

B.S., Materials Science and Engineering: June 2002
Nanjing University, Jiangsu, China

RESEARCH INTERESTS

Nonlinear optics, photonic structures and devices, meta-materials, modulators, optical antennas

RESEARCH EXPERIENCE

Research Assistant – Materials Science and Engineering, University of Washington, 2006–present

- Developed the first platform to efficiently pole electro-optic polymers using pyroelectric effect instead of conventional power source.
- Demonstrated the first successful poling of nanoslot waveguide device using pyroelectric crystals, which opens the possibility to simultaneously activate thousands of nano EO devices on a silicon chip in one process. Results were published as a cover story of Advanced Materials. (*Advanced Materials,* 24: OP1. doi: 10.1002/adma.201290057.)
- First to explain the importance of the space charge effect in the EO polymer studies. Develop the first example to use a TiO_2 barrier layer to suppress the space charge accumulation, which significantly improved the poling efficiency of many highly polarizable EO polymers.

- Optimized the process conditions of EO polymers in a variety of novel photonic devices, including high speed modulators, terahertz generators, electromagnetic wave detectors and on-chip optical interconnects.

Research Assistant – Materials Science & Engineering, Nanjing University, 2002–2005
- Independently developed the method to fabricate large area ferroelectric inverse opal photonic crystals through self-assemble approach. Characterized their structural and optical properties.

PATENTS

Poling structures and methods for producing electro-optic activity in organic nonlinear optical materials for electro-optic devices
United States Patent Application #: US20110091149
Inventors: Alex Kwan-yue Jen (advisor), Antao Chen (co-advisor), **Su Huang**, Jingdong Luo (group leader)

Phenyltetraene-based nonlinear optical chromophores
United States Patent Application #: US20100029953
Inventors: Alex Kwan-Yue Jen, Jingdong Luo, **Su Huang**, Yen-Ju Cheng, Tae-Dong Kim, Zhengwei Shi, Xinghua Zhou, Brent Polishak, Yanqing Tian

Diels-Alder crosslinkable dendritic nonlinear optic chromophores and polymer composites
United States Patent #: 8173045
Inventors: Alex Kwan-Yue Jen, Zhengwei Shi, Jingdong Luo, **Su Huang**, Xinghua Zhou

PEER-REVIEWED PUBLICATIONS

1. **Huang S**, Luo JD, Shi ZW, Zhou XH and Jen AKY, *Enhanced temporal stability of highly efficient guest-host electro-optic polymers through a barrier layer-assisted poling process*, **Journal of Materials Chemistry**, accepted.

2. **Huang S**, Luo JD, Yip HL, Ayazi A, Zhou XH, Gould M, Chen A, Baehr-Jones T, Hochberg M, Jen AKY, *Efficient Poling of Electro-Optic Polymers in Thin Films and Silicon Slot Waveguides by Detachable Pyroelectric Crystals,* **Advanced Materials**, 2012, 24, OP42–OP47. doi: 10.1002/adma.201102874; Cover story, **Advanced Materials,** 24: OP1. doi: 10.1002/adma.201290057.

3. **Huang S**, Kim TD, Luo JD, Hau SK, Shi ZW, Zhou XH, Yip HL, Jen AKY, *Highly efficient electro-optic polymers through improved poling using a thin TiO2-modified transparent electrode*, **Applied Physics Letters,** 2010, 96, 243311.

4. **Huang S**, Li AD, Gao Y, Wu D, Preparation and characterization of PLZT ferroelectric inverse opal, **International Journal of Modern Physics B**, 2005, 19,2769-2774.

5. Polishak BM, **Huang S**, Luo JD, Shi ZW, Zhou XH, Hsu A, Jen AKY, *A Triptycene-Containing Chromophore for Improved Temporal Stability of Highly Efficient Guest-Host Electrooptic Polymers*, **Macromolecules**, 2011, 44, 1261-1265.

6. Luo JD, **Huang S**, Shi ZW, Polishak BM, Zhou XH, Jen AKY, *Tailored Organic Electro-optic Materials and Their Hybrid Systems for Device Applications*, **Chemistry of Materials**, 2010, 23, 544-553.

7. Luo JD, **Huang S**, Cheng YJ, Kim TD, Shi ZW, Zhou XH, Jen AKY, *Phenyltetraene-based nonlinear optical chromophores with enhanced chemical stability and electro-optic activity*, **Organic Letters**, 2007, 9, 4471-4474.

8. Wu D, **Huang S**, Shao QY, Li AD, Ming NB, Ferroelectric $SrBi_2Ta_2O_9$-SiO_2 glass-ceramic thin films in metal/ferroelectric/insulator/semiconductor structures, **Physica Status Solidi a-Applied Research**, 2002, 193, R4-R6.

9. Shi ZW, Cui YZ, **Huang S**, Li ZA, Luo JD, and Jen AKY, *Dipolar Chromophore Facilitated Huisgen Cross-Linking Reactions for Highly Efficient and Thermally Stable Electrooptic Polymers*, **ACS Macro Letters**, 2012, 7, 793-796.

10. Shi ZW, Luo JD , **Huang S**, Polishak BM, Zhou XH, Liff S, Younkin TR, Block BA and Jen AKY, *Achieving excellent electro-optic activity and thermal stability in poled polymers through an expeditious crosslinking process*, ***Journal of Material Chemistry***, 2012, 22, 951-959.

11. Zhou XH, Luo JD, **Huang S**, Kim TD, Shi ZW, Cheng YJ, Jang SH, Knorr DB, Overney RM, Jen AKY, *Supramolecular Self-Assembled Dendritic Nonlinear Optical Chromophores: Fine-Tuning of Arene-Perfluoroarene Interactions for Ultralarge Electro-Optic Activity and Enhanced Thermal Stability*, **Advanced Materials**, 2009, 21, 1976-1981.

12. Shi ZW, Luo JD, **Huang S**, Cheng YJ, Kim TD, Polishak BM, Zhou XH, Tian YQ, Jang SH, Knorr DB, Overney RM, Younkin TR, Jen AKY, *Controlled Diels-Alder Reactions Used To Incorporate Highly Efficient Polyenic Chromophores into Maleimide-Containing Side-Chain Polymers for Electro-Optics*, **Macromolecules**, 2009, 42, 2438-2445.

13. Cheng YJ, Luo JD, **Huang S**, Zhou XH, Shi ZW, Kim TD, Bale DH, Takahashi S, Yick A, Polishak BM, Jang SH, Dalton LR, Reid PJ, Steier WH, Jen AKY, *Donor-acceptor thiolated polyenic chromophores exhibiting large optical nonlinearity and excellent photostability*, **Chemistry of Materials**, 2008, 20, 5047-5054.

14. Shi ZW, Luo JD, **Huang S**, Zhou XH, Kim TD, Cheng YJ, Polishak BM, Younkin TR, Block BA, Jen AKY, *Reinforced Site Isolation Leading to Remarkable Thermal Stability and High Electrooptic Activities in Cross-Linked Nonlinear Optical Dendrimers*, **Chemistry of Materials**, 2008, 20, 6372-6377.

15. Li AD, Wang YJ, **Huang S**, Cheng JB, Wu D, Ming NB, Effect of in situ applied electric field on the growth of La2Ti2O7 thin films by chemical solution deposition, Journal of Crystal Growth, 2004, 268, 198-203.

16. Zhou XH, Luo JD, Joshua DA, **Huang S**, Jen AKY, *Push-pull tetraene chromophores derived from dialkylaminophenyl, tetrahydroquinolinyl and julolidinyl moieties: optimization of second-order optical nonlinearity by fine-tuning the strength of electron-donating groups*, ***Journal of Material Chemistry***, 2012, **DOI:** 10.1039/C2JM32848H. First published on web Jun 13, 2012.

17. Gould M, Baehr-Jones T, Ding R, **Huang S**, Luo JD, Jen AKY, Fedeli JM, Fournier M, Hochberg M, *Silicon-polymer hybrid slot waveguide ring-resonator modulator*, **Optics Express**, 2011, 19, 3952-3961.

18. Shi ZW, Liang W, Luo JD, **Huang S**, Polishak BM, Li XS, Younkin TR, Block BA, Jen AKY, *Tuning the Kinetics and Energetics of Diels-Alder Cycloaddition Reactions to improve Poling Efficiency and Thermal Stability of High-Temperature Cross-Linked Electro-Optic Polymers*, **Chemistry of Materials,** 2010, 22, 5601-5608.

19. McLaughlin CV, Hayden LM, Polishak B, **Huang S**, Luo JD, Kim TD, Jen AKY, Wideband 15 THz response using organic electro-optic polymer emitter-sensor pairs at telecommunication wavelengths, **Applied Physics Letters, 2008,** 92, 151107.

20. Liu WC, Li AD, Tan J, **Huang S**, Wu D, Shen ZR, Ye H, Ming NB, Preparation and electro-optic properties of poled nanocrystals and polymer composite BaTiO3/PC films, **Ferroelectrics**, 2005, 329, 983-987.

21. Ding R, Baehr-Jones T, Liu Y, Bojko R, Witzens J, **Huang S**, Luo JD, Benight S, Sullivan P, Fedeli JM, Fournier M, Dalton L, Jen AKY, Hochberg M, *Demonstration of a low V_{pi}-L modulator with GHz bandwidth based on electro-optic polymer-clad silicon slot waveguides*, **Optics Express**, 2010, 18, 15618-15623.

22. Block BA, Younkin TR, Davids PS, Reshotko MR, Chang P, Polishak BM, **Huang S**, Luo JD, Jen AKY, *Electro-optic polymer cladding ring resonator modulators*, **Optics Express**, 2008, 16, 18326-18333.

23. Tian YQ, Chen CY, Haller MA, Tucker NM, Ka JW, Luo JD, **Huang S**, Jen AKY, *Nanostructured functional block copolymers for electrooptic devices*, **Macromolecules**, 2007, 40, 97-104.

24. Ding R, Baehr-Jones T, Kim WJ, Spott A, Fournier M, Fedeli JM, **Huang S**; Luo JD; Jen AKY, Dalton L, Hochberg M, *Sub-Volt Silicon-Organic Electro-optic Modulator With 500 MHz Bandwidth*, **Journal of Lightwave Technology**, 2011, 8, 1112-1117.

25. Greenlee C, Guilmo A, Opadeyi A, Himmelhuber R, Norwood RA, Fallahi M, Luo JD, **Huang S**, Zhou XH, Jen AKY, Peyghambarian N, *Mach-Zehnder interferometry method for decoupling electro-optic and piezoelectric effects in poled polymer films*, **Applied Physics Letters**, 2010, 97, 041109.

26. Yi F, Ou F, Liu BY, Huang YY, Ho ST, Wang YL, Liu J, Marks TJ, **Huang S**, Luo JD, Jen AKY, Dinu R, Jin D, *Electro-optic modulator with exceptional power-size performance enabled by transparent conducting electrodes*, **Optics Express**, 2010, 18, 6779-6796.

27. Kim TD, Luo JD, Cheng YJ, Shi ZW, Hau S, Jang SH, Zhou XH, Tian Y, Polishak B, **Huang S**, Ma H, Dalton LR, Jen AKY, *Binary chromophore systems in nonlinear optical dendrimers and polymers for large electrooptic activities*, **Journal of Physical Chemistry C**, 2008, 112, 8091-8098.